Full-field identification of mixed-mode adhesion properties in microelectronics from micrographs only

Johan Hoefnagels,

Andre Ruybalid, Olaf van der Sluis, & Marc Geers

dept. Mechanical Engineering

Eindhoven University of Technology, NL

j.p.m.hoefnagels@tue.nl

www.tue.nl/hoefnagels-group

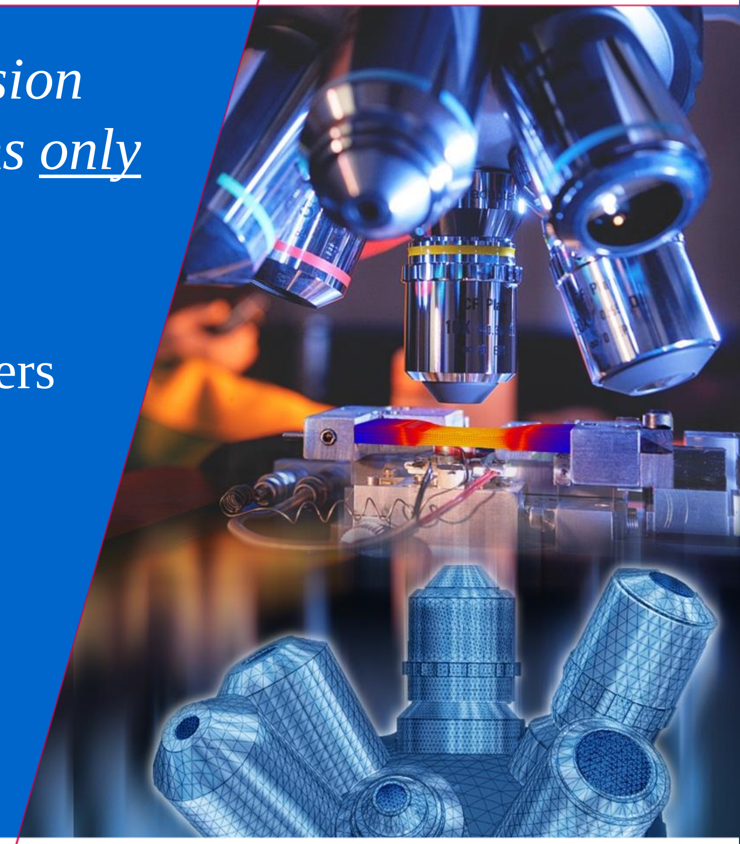

Where innovation starts

/ Mixed-mode interface identification from movie only

- Interface delamination in micro-electronics / microsystems / microstructures:

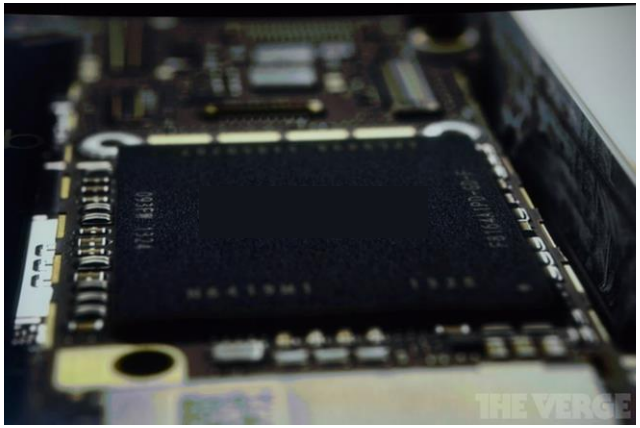

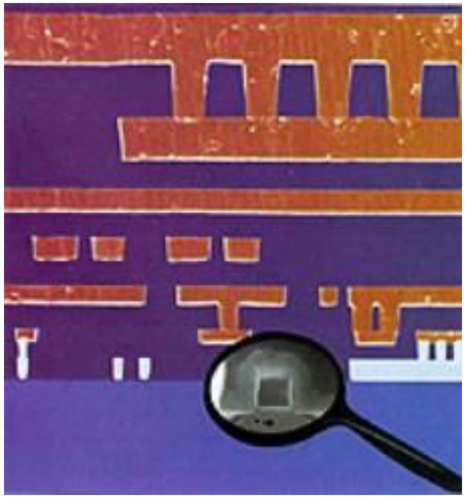

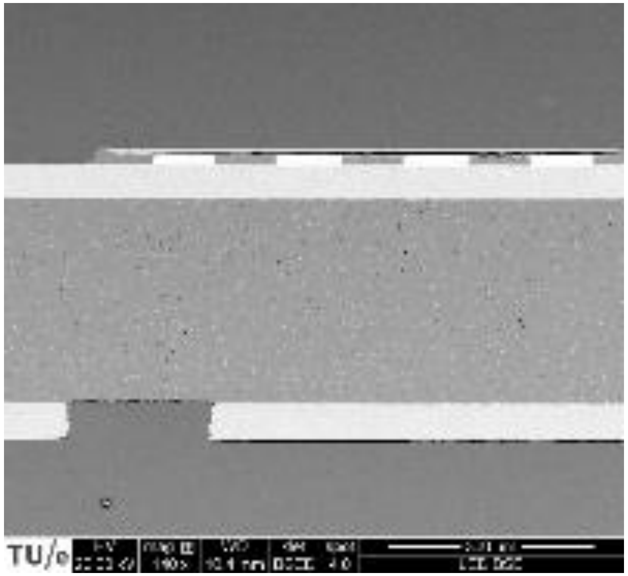

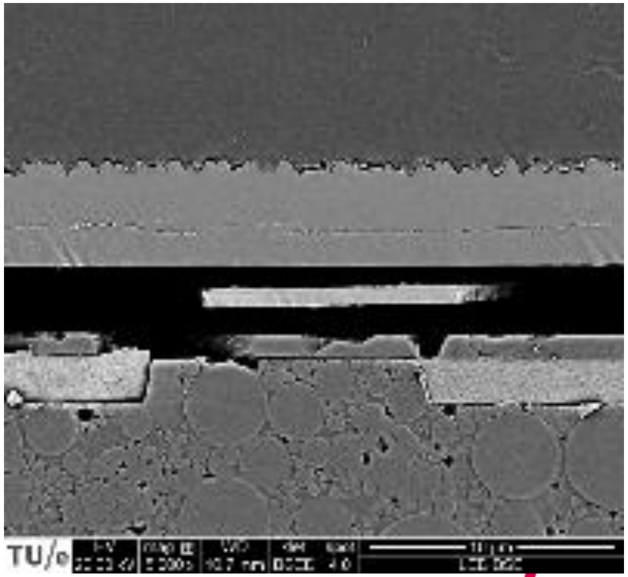

/ Mixed-mode interface identification from movie only

- Interface delamination in micro-electronics / microsystems / microstructures:
  - Challenging: interface behavior can only indirectly be measured through effect on adherent layers
  - Only Microscopic images: **NO** force measurement (!) + restricted field of view
    - physical Boundary Conditions not in view ➔ how to apply accurate local BC to mechanical model ?
  - Clean single-mode delamination test not possible ➔ large change of mode mixity during test

  ➔ opportunity!: identification of mixed-mode CZ model from single mixed-mode test

- Cohesive Zone (CZ)
  - Smith-Ferrante traction-separation law
    - 3 parameters: $G_{c,n}, G_{c,t}, \delta_c$

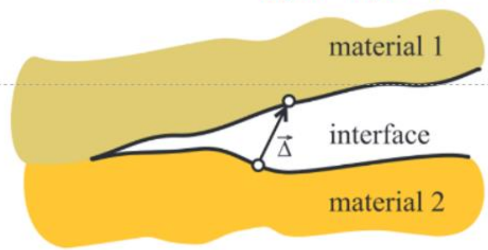

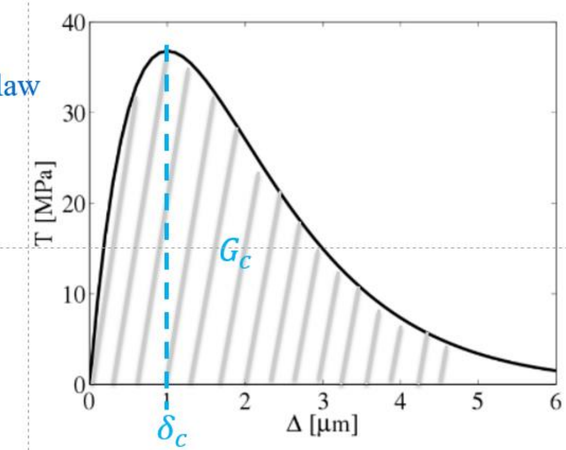

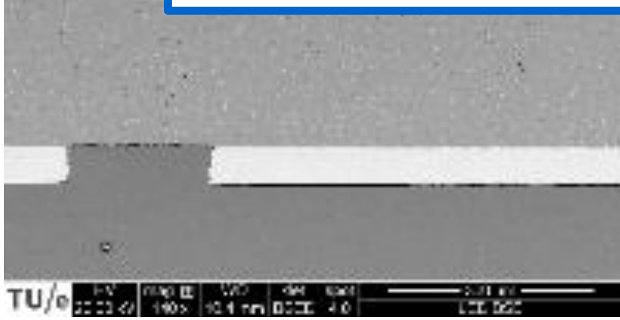

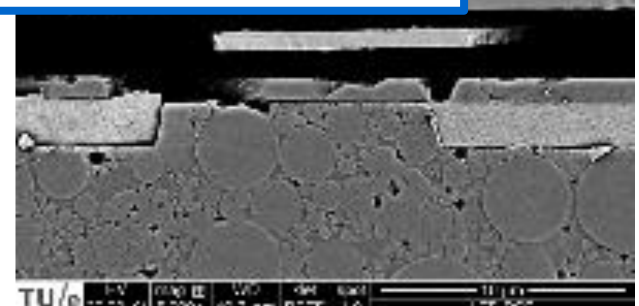

Technische Universiteit Eindhoven University of Technology

Brightness conservation:

$$r(\vec{x}) = f(\vec{x}) - g(\vec{x} + \vec{u}) \approx 0$$

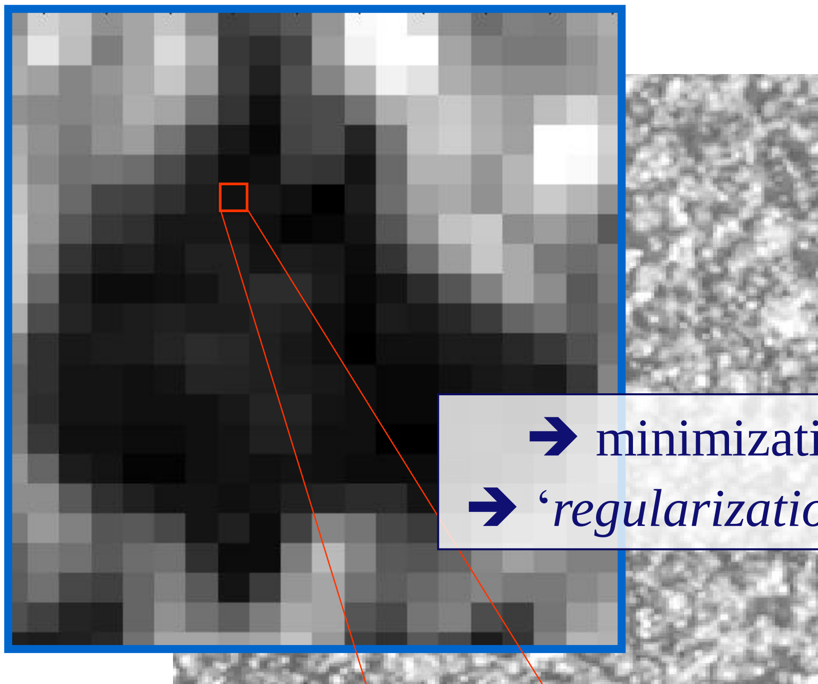

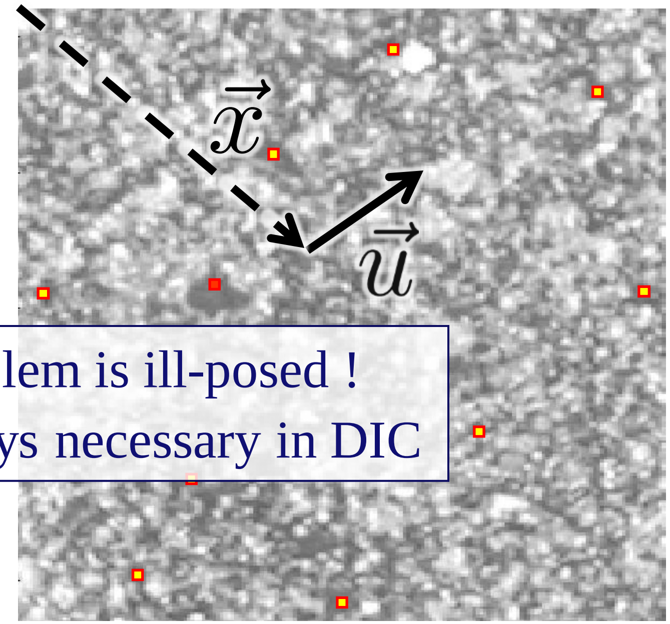

➔ minimization problem is ill-posed !

➔ '*regularization*' always necessary in DIC

f g

➔ Minimization of the residual 'averaged' over a region of interest Ω:

$$\Psi(\vec{u}) = \int_\Omega \{r(\vec{x})\}^2 d\vec{x} = \int_\Omega \{f(\vec{x}) - g(\vec{x} + \vec{u})\}^2 d\vec{x} \approx 0$$

- Choice of Regularization?

subset based ('**local DIC**')

subset matching

matching of entire image

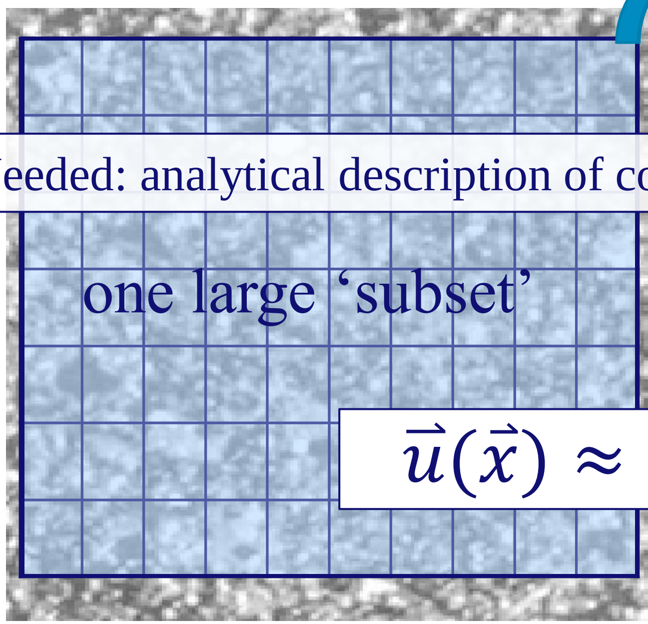

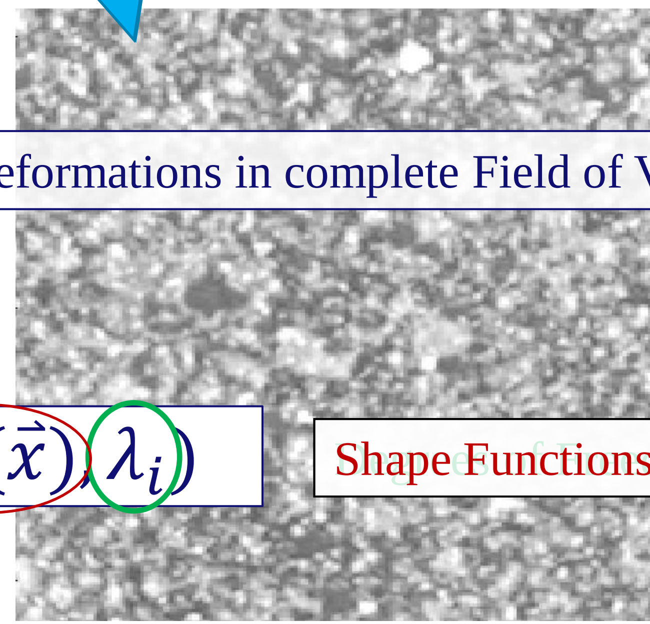

➔ Needed: analytical description of complex deformations in complete Field of View

$$\vec{u}(\vec{x}) \approx \vec{u}(\vec{\varphi}_i(\vec{x}), \lambda_i)$$

Shape Functions

Degrees of Freedom

f

➔ Minimization of the residual 'averaged' over a region of in

e.g.: polynomial basis:

$$\vec{u} \approx \lambda_1 x^0 y^0 + \lambda_2 x^1 y^0 + \lambda_3 x^2 y^0 + \ldots$$

$$\vec{\varphi}_i \approx \frac{\partial \vec{u}}{\partial \lambda_i}$$

Cheng et al. ExpMech(2002); Sun et al. AppOpt(2005); Besnard et al. ExpMech(2006); …

/ Global DIC: choice of shape functions

Examples of 2D (continuous) basis functions for Global DIC

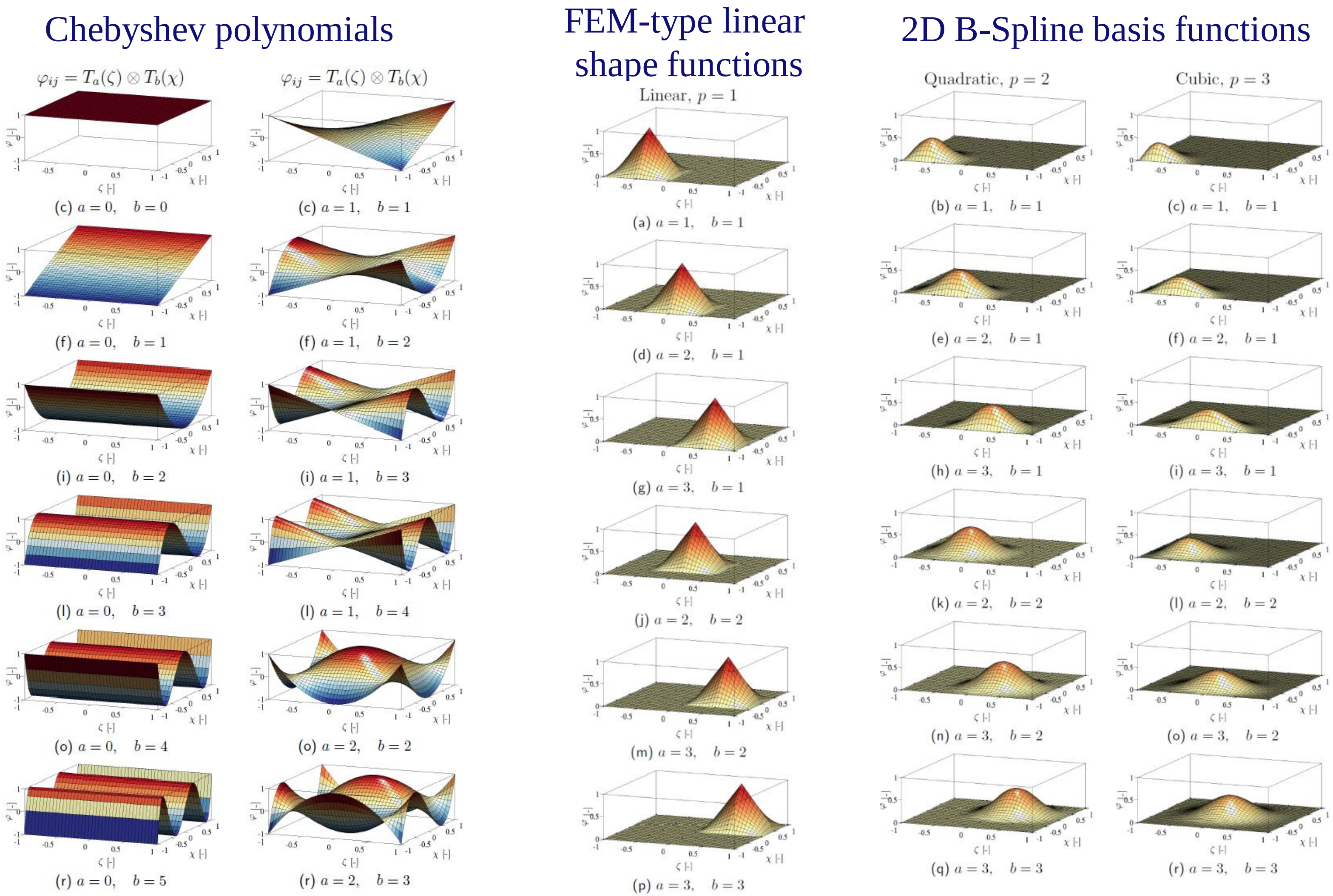

Neggers et al., Exp. Mech. 47, 717 (2014); Negger et al., IJNME 105, 243–260 (2015)

/ Integrated DIC: physically motivated model for $\vec{u}(\vec{x}, \lambda_i)$

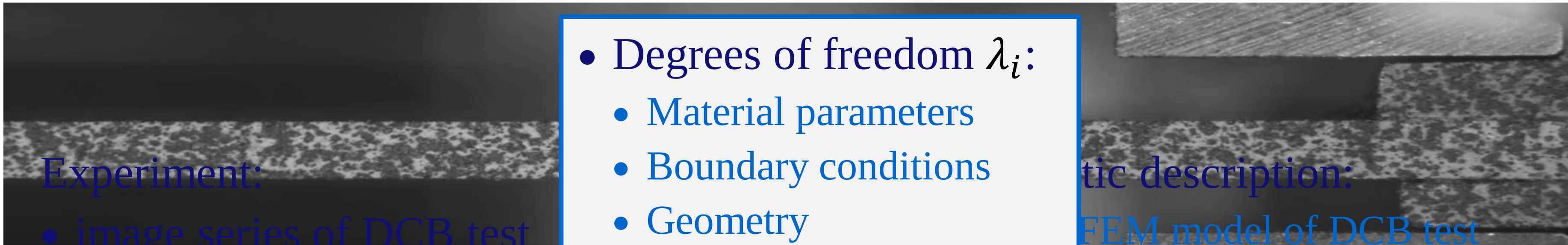

Experiment:

- image series of DCB test

tic description:

- FEM model of DCB test

- Degrees of freedom λ_i:
  - Material parameters
  - Boundary conditions
  - Geometry
  - ….

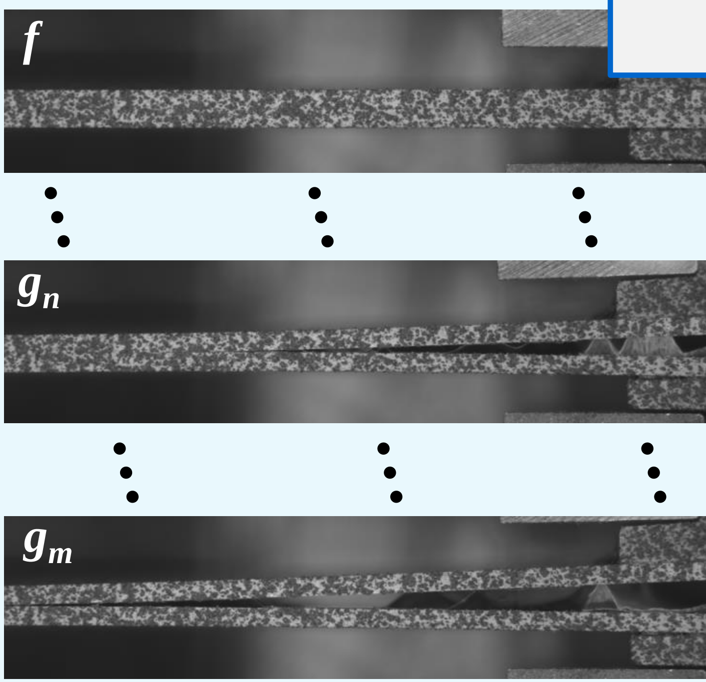

IDIC

$\lambda_i + \Delta\lambda_i$

$$\boxed{\varphi_i = \frac{\partial \vec{u}}{\partial \lambda_i}}$$

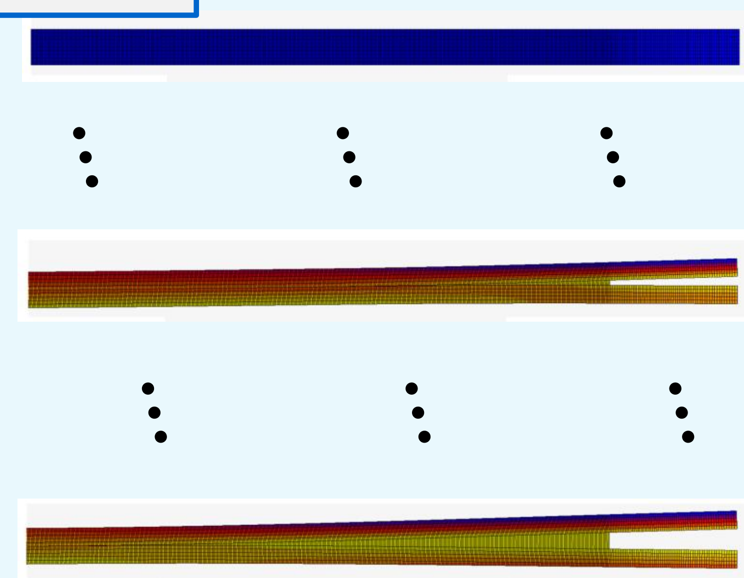

$$\vec{u} = \vec{u}(\vec{x}, t, \lambda_i)$$

Roux *et al.* IJF(2006), Rethore *et al.* EJCS(2009); IJSS(2013); Neggers *et al.* IJNME(2015)

/ Integrated DIC: physically motivated model for $\vec{u}(\vec{x}, \lambda_i)$

Experiment:

- image series of DCB test

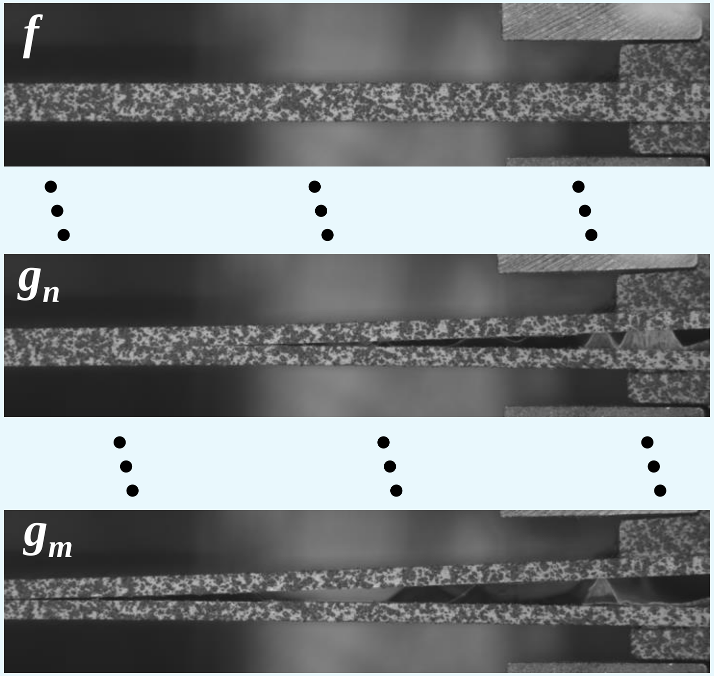

IDIC

+

Kinematic description:

- e.g. ***analytical*** model

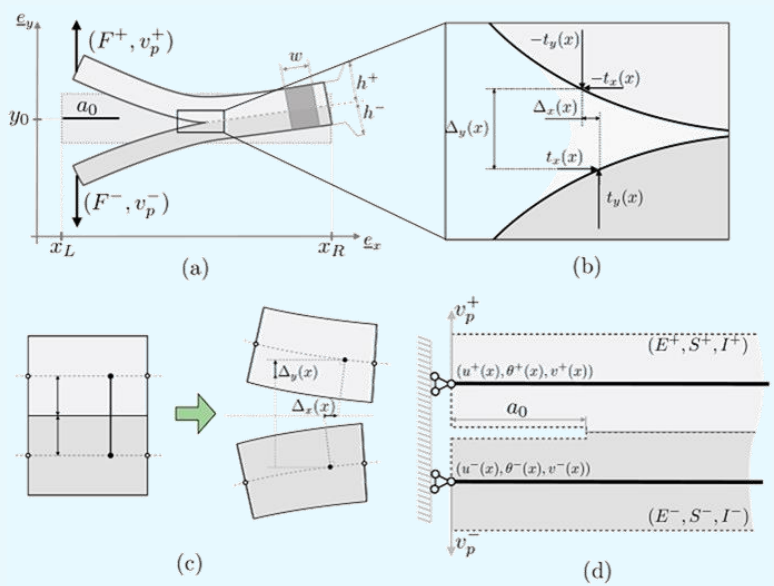

Blaysat, *et al.*, Int.J.Solids.Struct. (2015)

$$\vec{u} = \vec{u}(\vec{x}, t, \lambda_i)$$

Roux *et al.* IJF(2006), Rethore *et al.* EJCS(2009); IJSS(2013); Neggers *et al.* IJNME(2015)

/ Integrated DIC: physically motivated model for $\vec{u}(\vec{x}, \lambda_i)$

Experiment:

- image series of DCB test

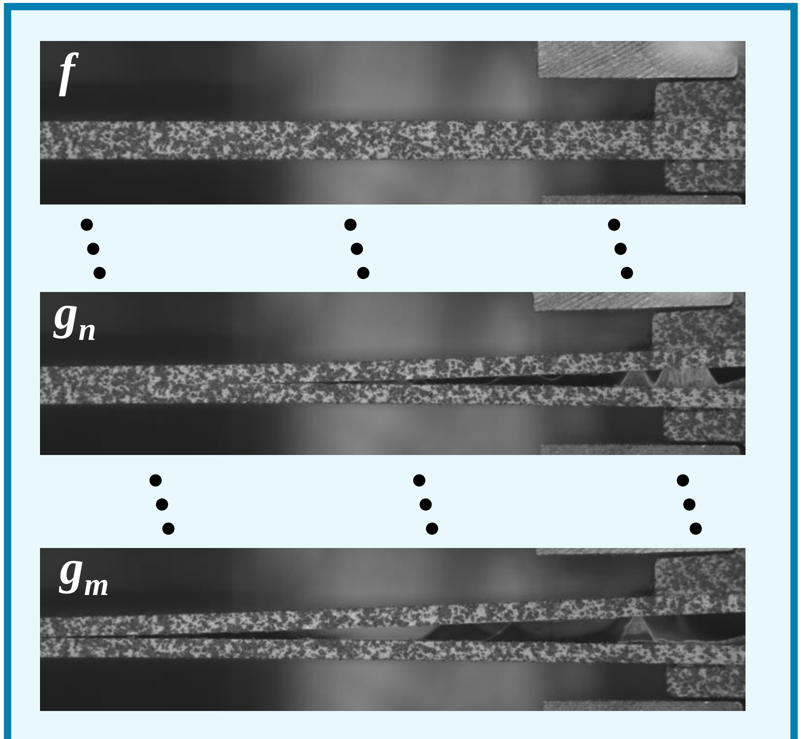

IDIC

Kinematic description:

- e.g. FEM model of DCB test

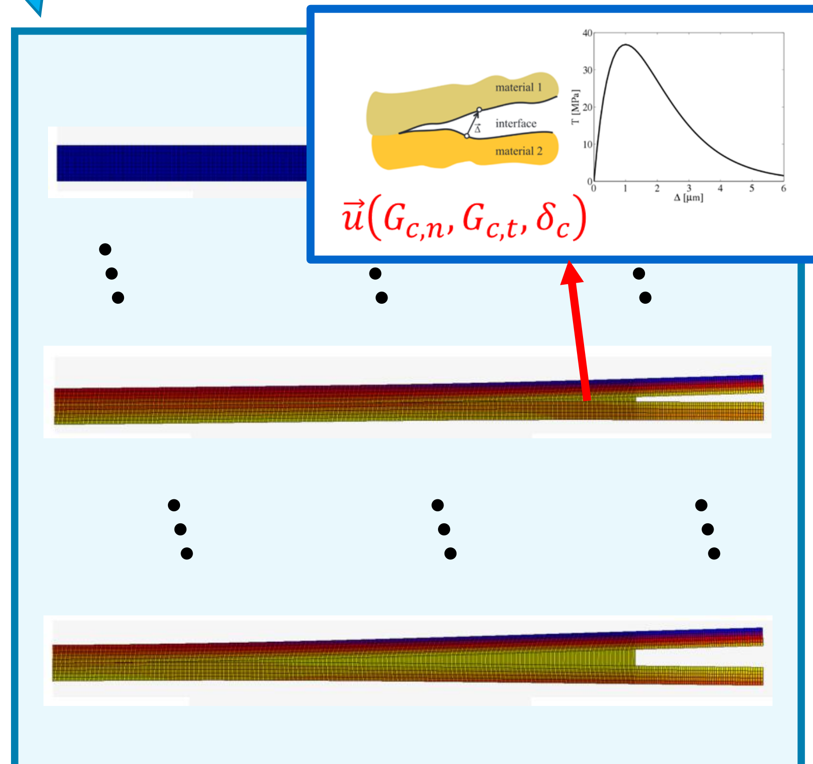

$$\vec{u} = \vec{u}(\vec{x}, t, \lambda_i)$$

Roux *et al.* IJF(2006), Rethore *et al.* EJCS(2009); IJSS(2013); Neggers *et al.* IJNME(2015)

/ Comparison: FEMU vs. IDIC

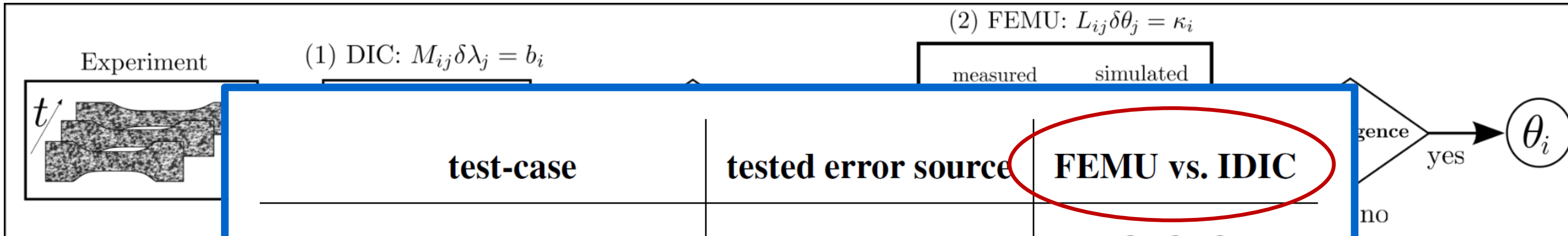

- FEMU =
  (1) DIC y
  (2) par. ic

(1993); …

test-case	tested error source	FEMU vs. IDIC
1	systematic errors	○ ● ○
2 elastoplastic	poor initial guess	○ ● ○
3 (large deformation)	modeling error	○ ● ○
4	image noise	○ ○ ●
5	systematic errors	○ ○ ●
6 cubic orthotropic elastic	poor initial guess	○ ● ○
7 (small deformation)	modeling error	○ ● ○
8	image noise	○ ○ ●
9 higher complexity	DIC subset size	○ ○ ●

Ruybalid *et al.*, IJNME (2015) ➔ Hild & Roux, IJSS (2020)

- IDIC =
  (1) direct parameter identification
  by matching the images

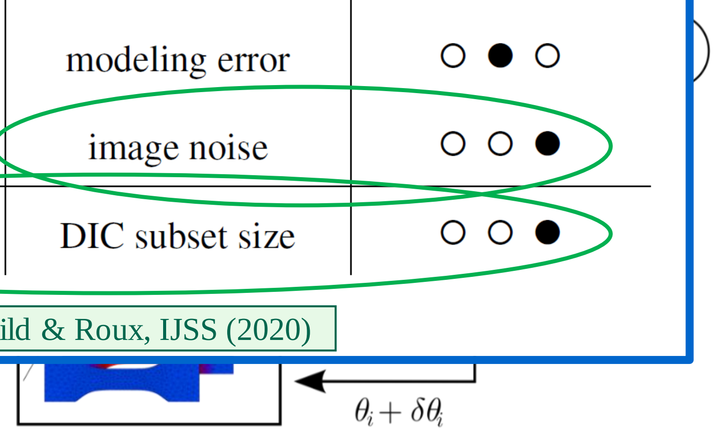

Roux *et al.* IJF(2006), Rethore *et al.* EJCS(2009); IJSS(2013); Neggers *et al.* IJNME(2015); Neggers *et al.* IJSS(20165); . . .

/ Mixed-mode interface identification from movie only

- Interface delamination in micro-electronics / microsystems / microstructures:
  - Challenging: interface behavior can only indirectly be measured through effect on adherent layers
  - Only Microscopic images: **NO** force measurement (!) + restricted field of view
    - physical Boundary Conditions <u>not</u> in view ➔ how to apply accurate <u>local</u> BC to mechanical model ?
  - Clean single-mode delamination test not possible ➔ large change of mode mixity during test

  ➔ opportunity!: identification of mixed-mode CZ model from single mixed-mode test, from movie only

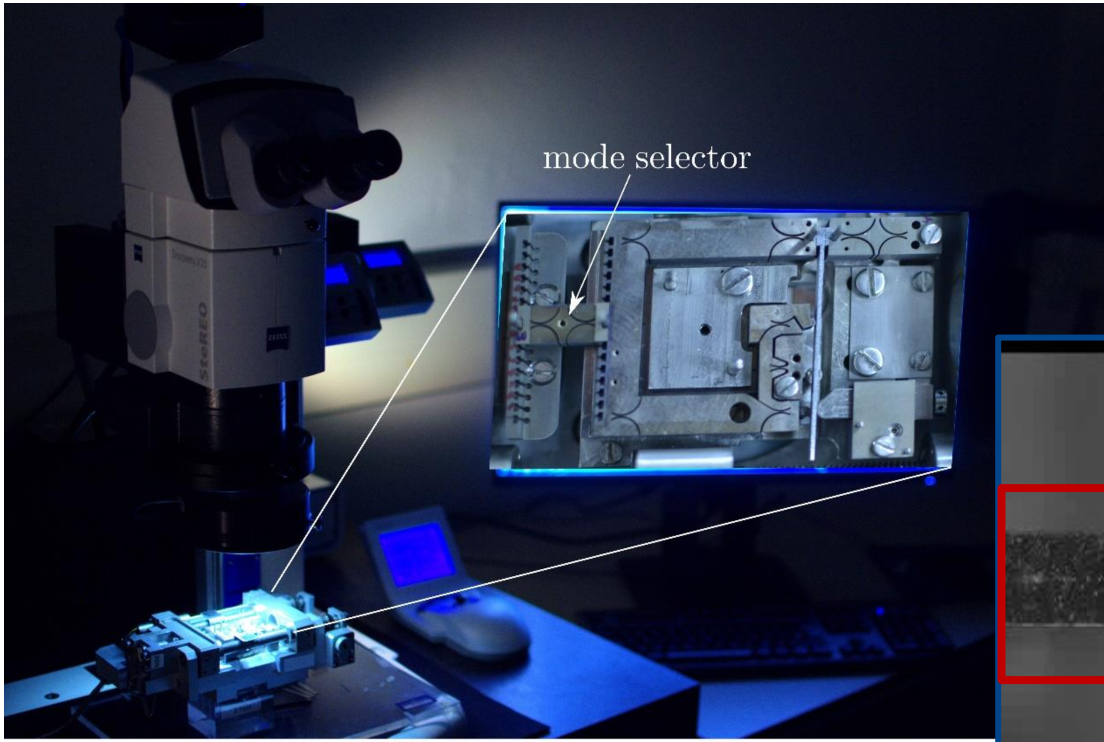

(a) MMMB setup under the microscope

- Model system:
  - Bi-layer specimen with single interface
  - "Miniature Mixed-Mode Bending setup" under in-situ optical microscopy

Kolluri et al. IJF (2009); Kolluri et al. J.Phys.D (2010); Kolluri et al. IJF (2013)

- Interface delamination in micro-electronics / microsystems / microstructures:

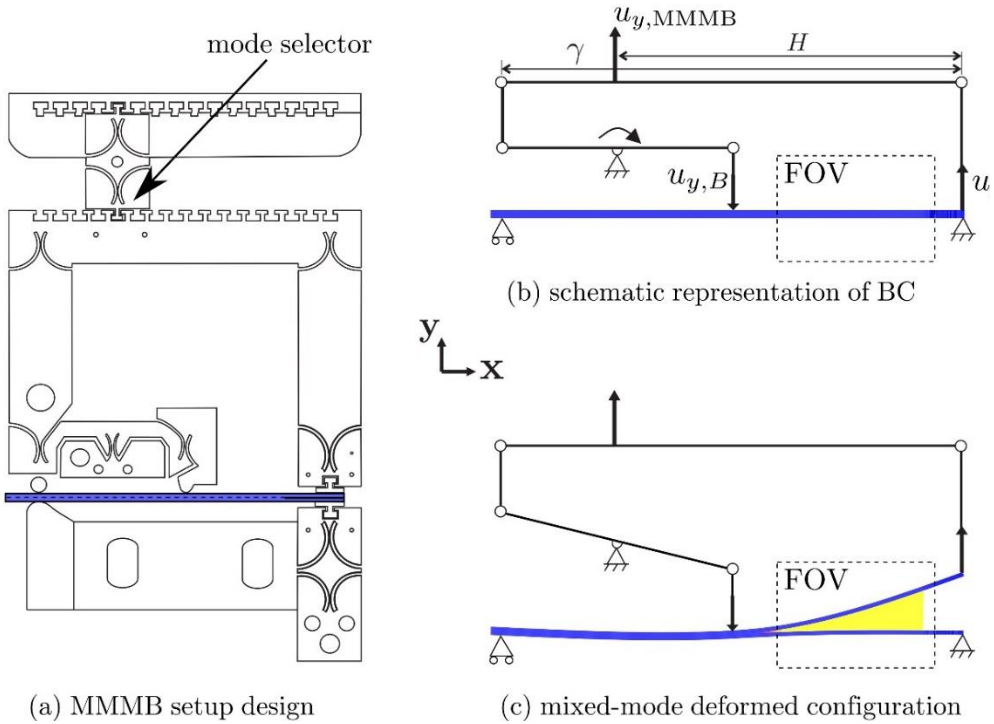

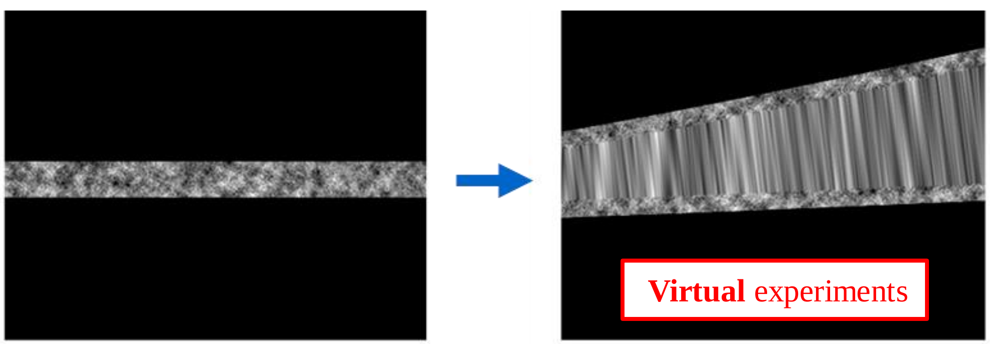

- Model system:
  - Bi-layer specimen with single interface
  - “Miniature Mixed-Mode Bending setup” under in-situ optical microscopy
  - Virtual simulation of MMMB

Kolluri et al. IJF (2009); Kolluri et al. J.Phys.D (2010); Kolluri et al. IJF (2013)

/ Mode I: Local Boundary Conditions

Virtual experiments

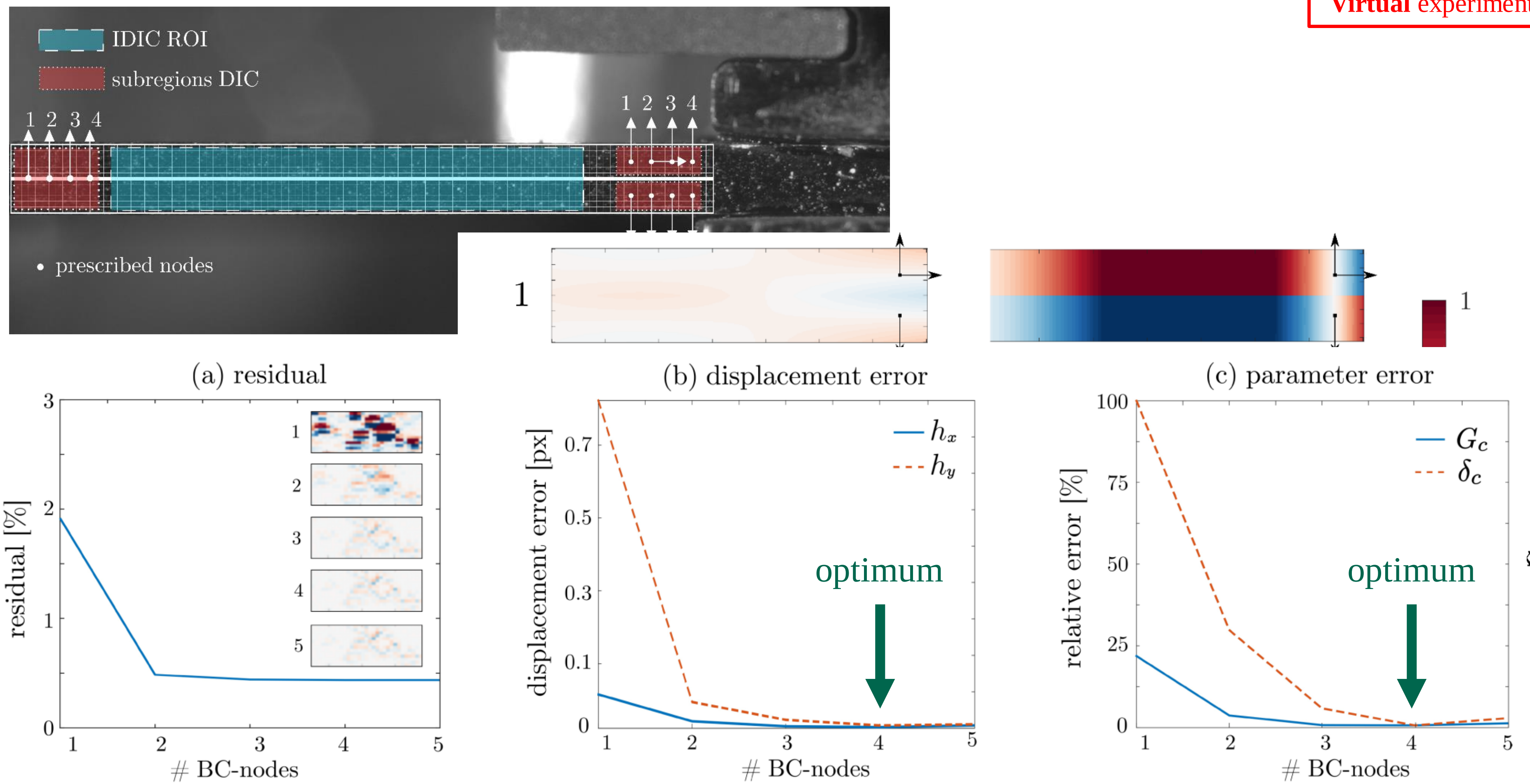

- Local boundary conditions (no force correlation):
  - Capture kinematics accurately
  - ROI: sufficient unconstrained region

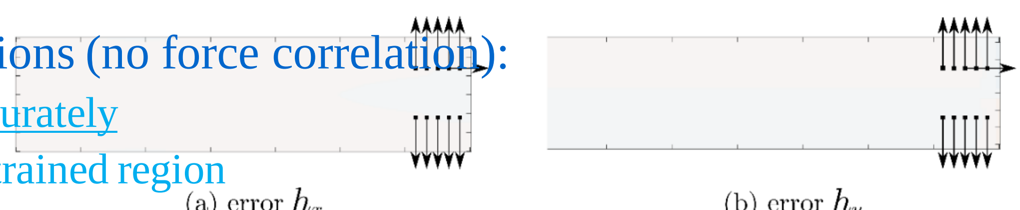

Ruybalid, Hoefnagels, v.d. Sluis, Geers, IJSS, 2017

/ Mode I: Experimental results

Real experiments

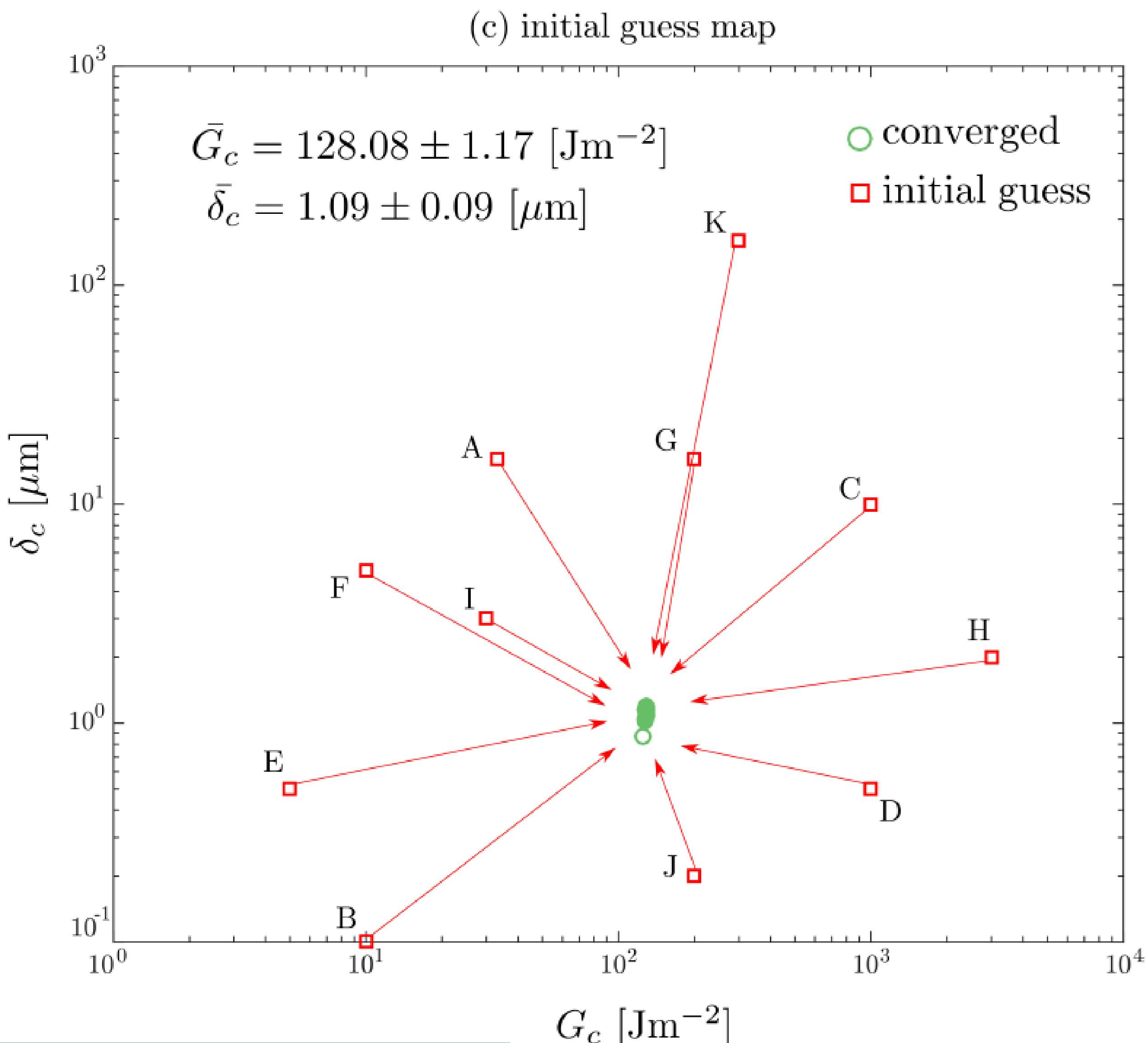

Ruybalid, Hoefnagels, v.d. Sluis, Geers, IJSS, 2017

/ Mixed-mode: Local Boundary conditions

Virtual experiments

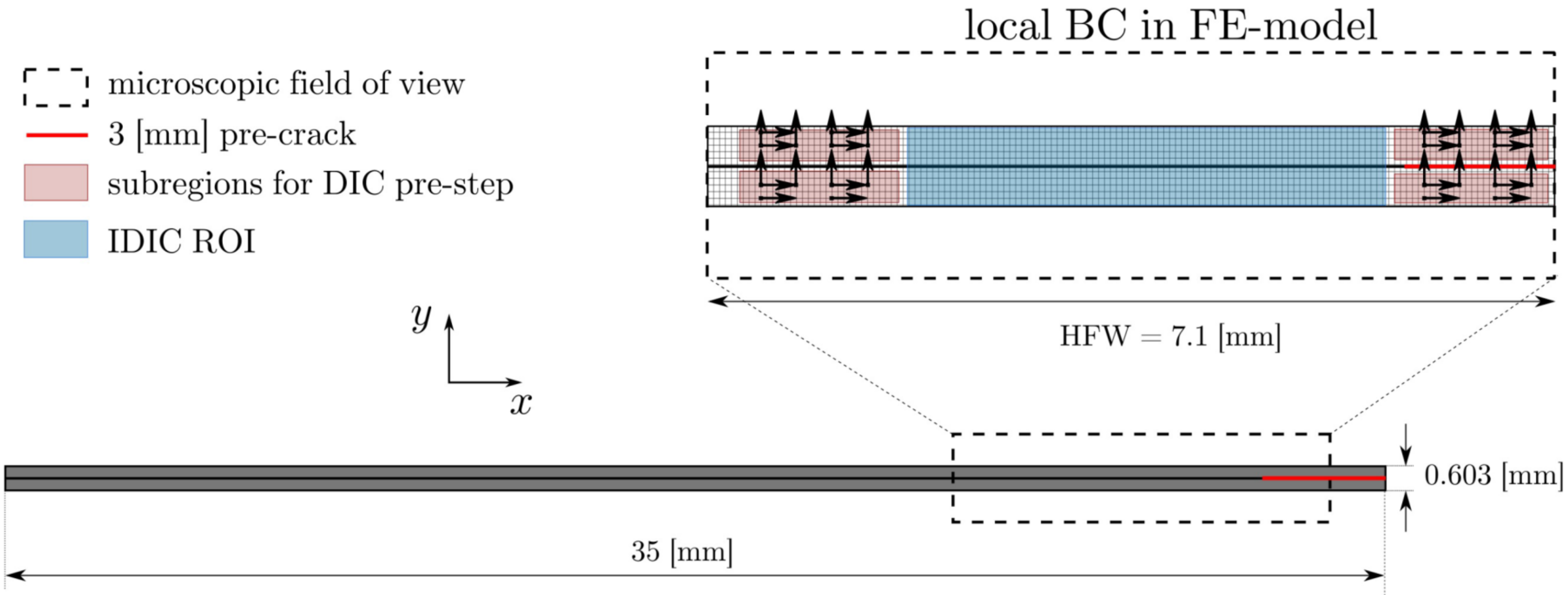

e.g.: simulation of mode-mixity: $\zeta = 0.6$ (~70°) *(10x deformations)*

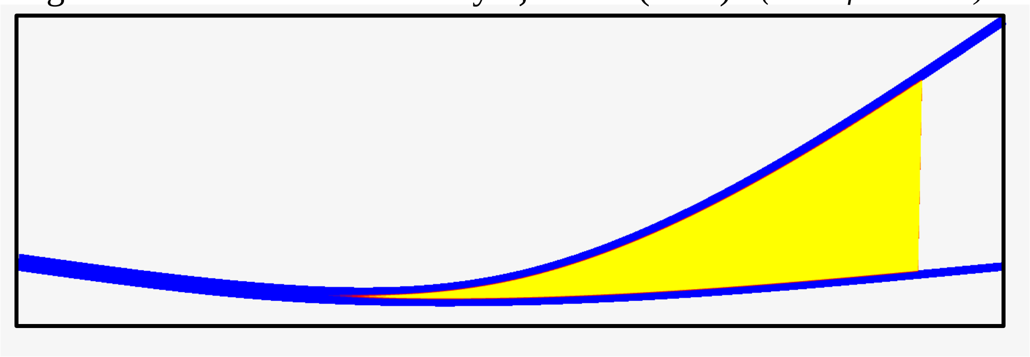

Virtual experiments

Different mode-mixity: $\xi = 0.0, 0.2, 0.4, 0.5, 0.6, 0.7, 0.75$

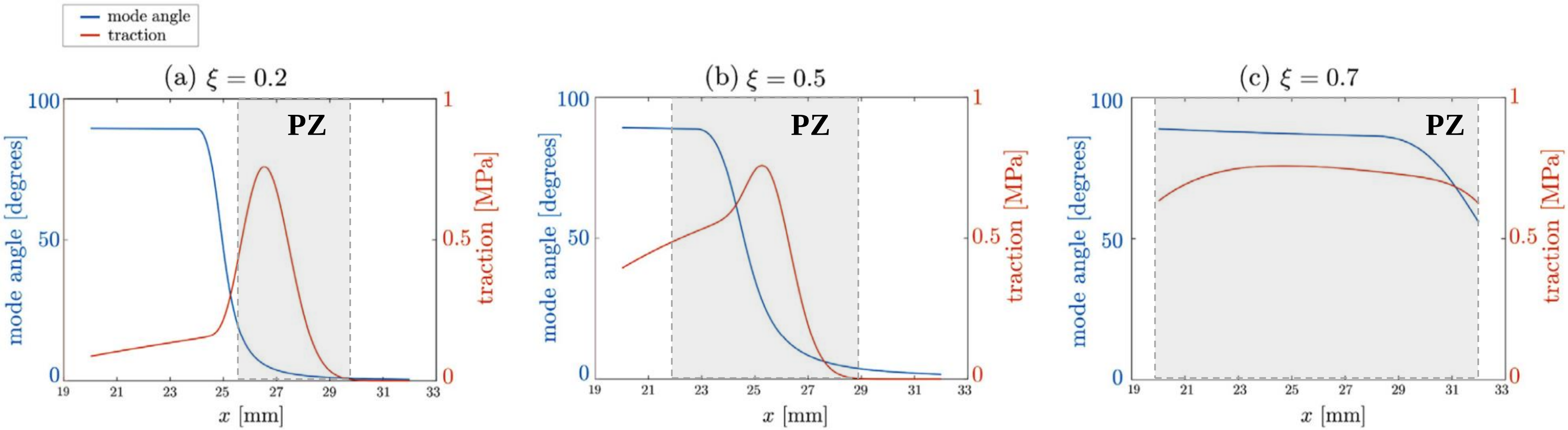

e.g.: simulation of m... ξ = 0.6 (~70°) *(10x deformations)*

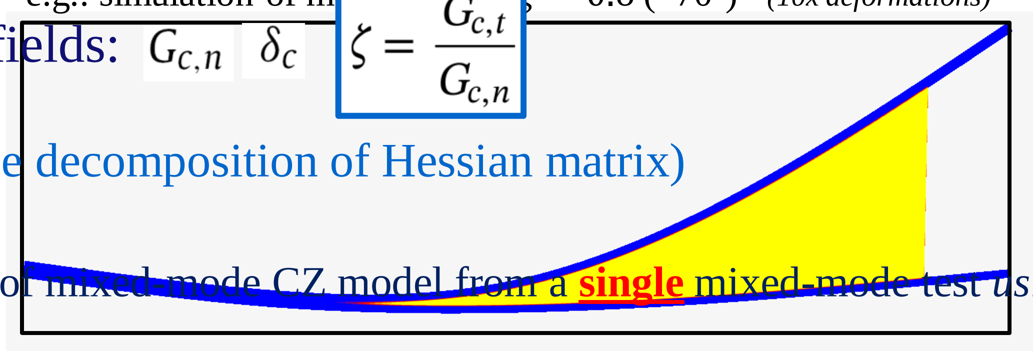

- Sensitivity fields: $G_{c,n}$ δ_c
  - (eigen value decomposition of Hessian matrix)

$$\zeta = \frac{G_{c,t}}{G_{c,n}}$$

➔ identification of mixed-mode CZ model from a **single** mixed-mode test *using micrographs only* ?

Ruybalid, Hoefnagels, v.d. Sluis, Geers, IJSS, 2018

Virtual experiments

Different mode-mixity: $\xi = 0.0, 0.2, 0.4, 0.5, 0.6, 0.7, 0.75$

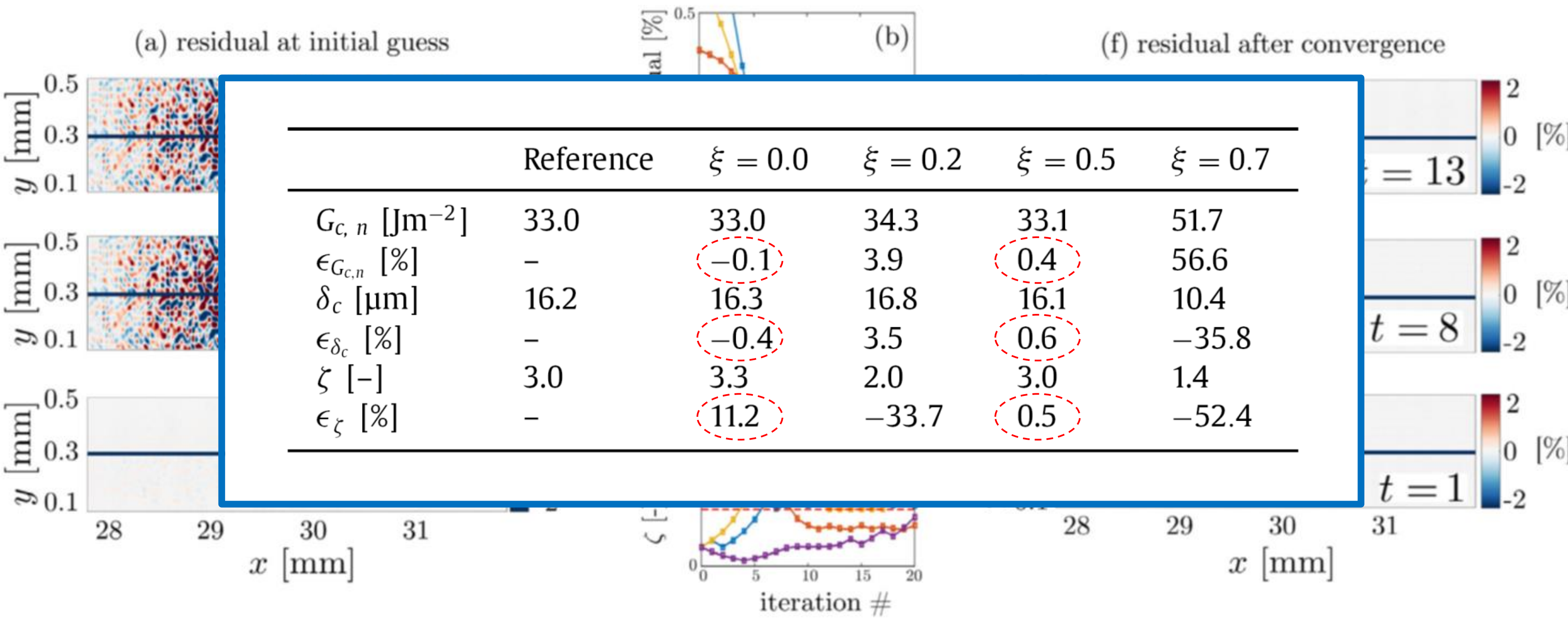

	Reference	$\xi = 0.0$	$\xi = 0.2$	$\xi = 0.5$	$\xi = 0.7$
$G_{c,\,n}$ [$\mathrm{Jm^{-2}}$]	33.0	33.0	34.3	33.1	51.7
$\epsilon_{G_{c,n}}$ [%]	–	−0.1	3.9	0.4	56.6
δ_c [μm]	16.2	16.3	16.8	16.1	10.4
ϵ_{δ_c} [%]	–	−0.4	3.5	0.6	−35.8
ζ [–]	3.0	3.3	2.0	3.0	1.4
ϵ_{ζ} [%]	–	11.2	−33.7	0.5	−52.4

➔ identification of mixed-mode CZ model from a **single** mixed-mode test *using micrographs only* !

Ruybalid, Hoefnagels, v.d. Sluis, Geers, IJSS, 2018

/ Mixed-mode: Virtual Experiments

Virtual experiments

Different mode-mixity: $\xi = 0.0, 0.2, 0.4, 0.5, 0.6, 0.7, 0.75$

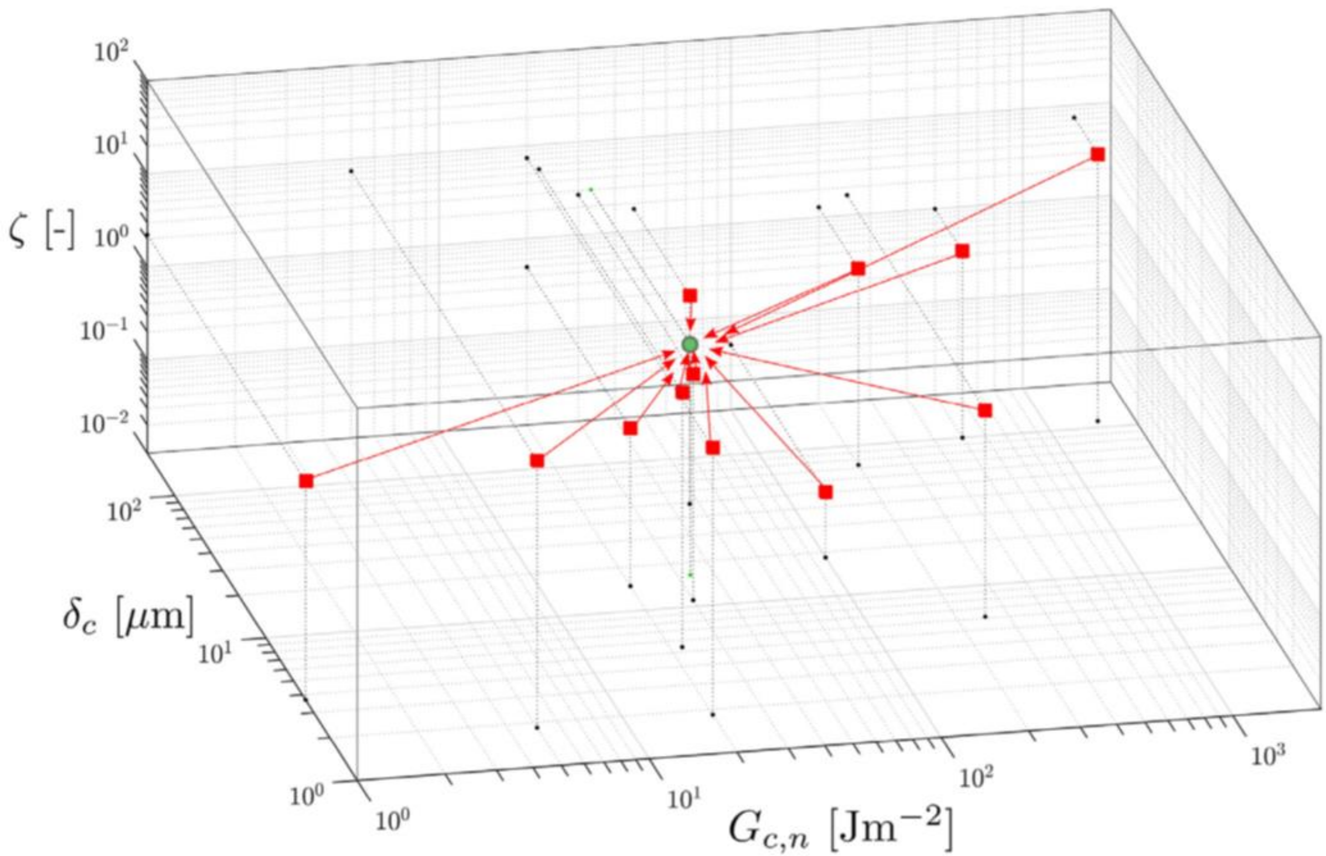

➔ identification of mixed-mode CZ model from a **single** mixed-mode test *using micrographs only* !

/ Mixed-mode: Real Experiments

Real experiments

Different mode-mixity: ξ = 0.0, 0.25, 0.5, 0.63

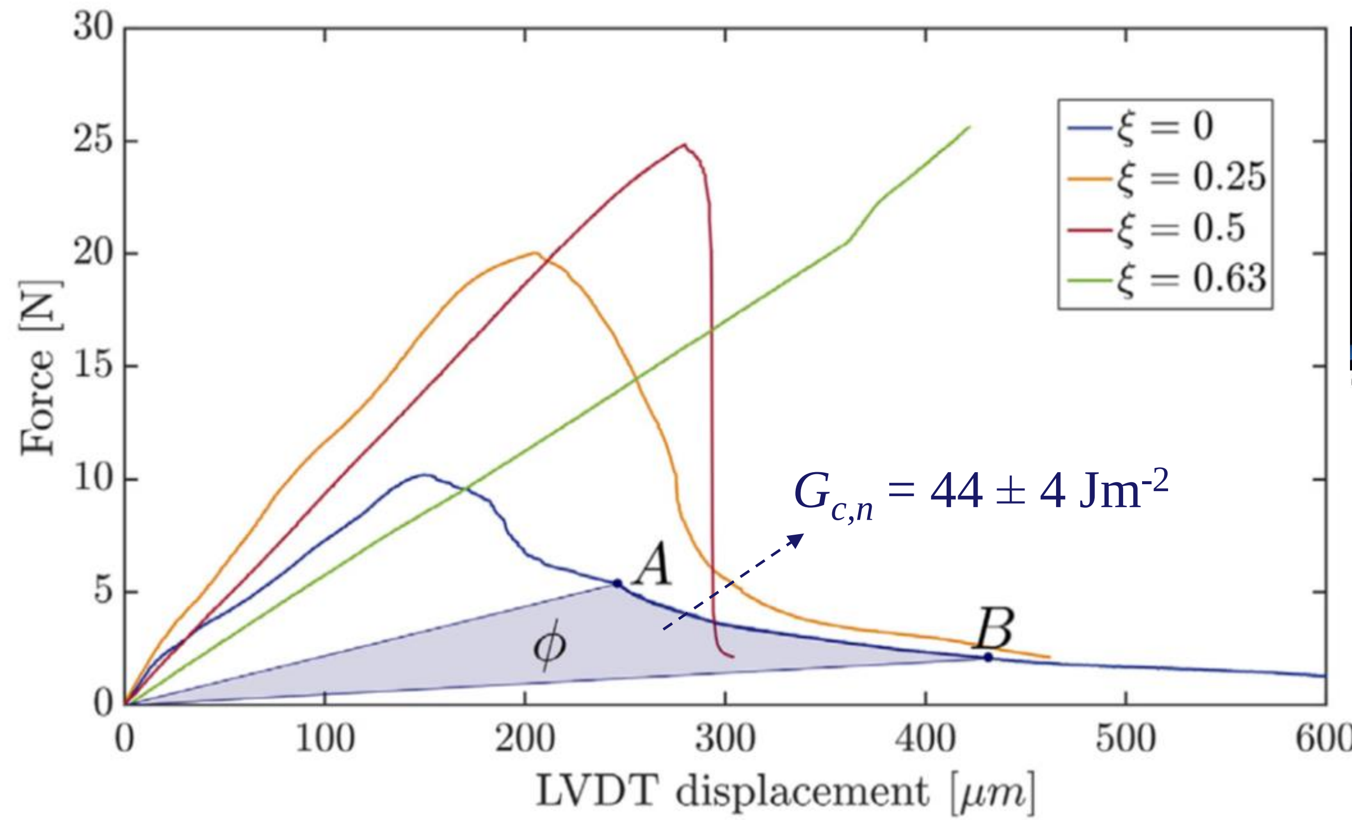

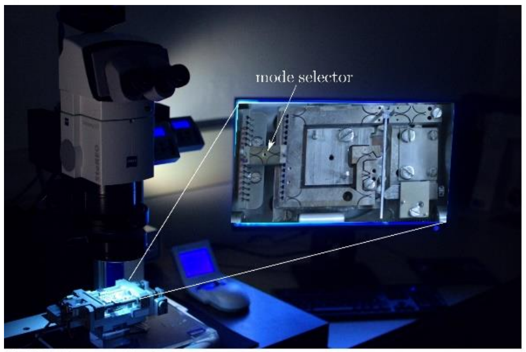

(a) MMMB setup under the microscope

➔ identification of mixed-mode CZ model from a **single** mixed-mode test *using micrographs only* ?

Real experiments

Different mode-mixity: $\xi = 0.0, 0.25, 0.5, 0.63$

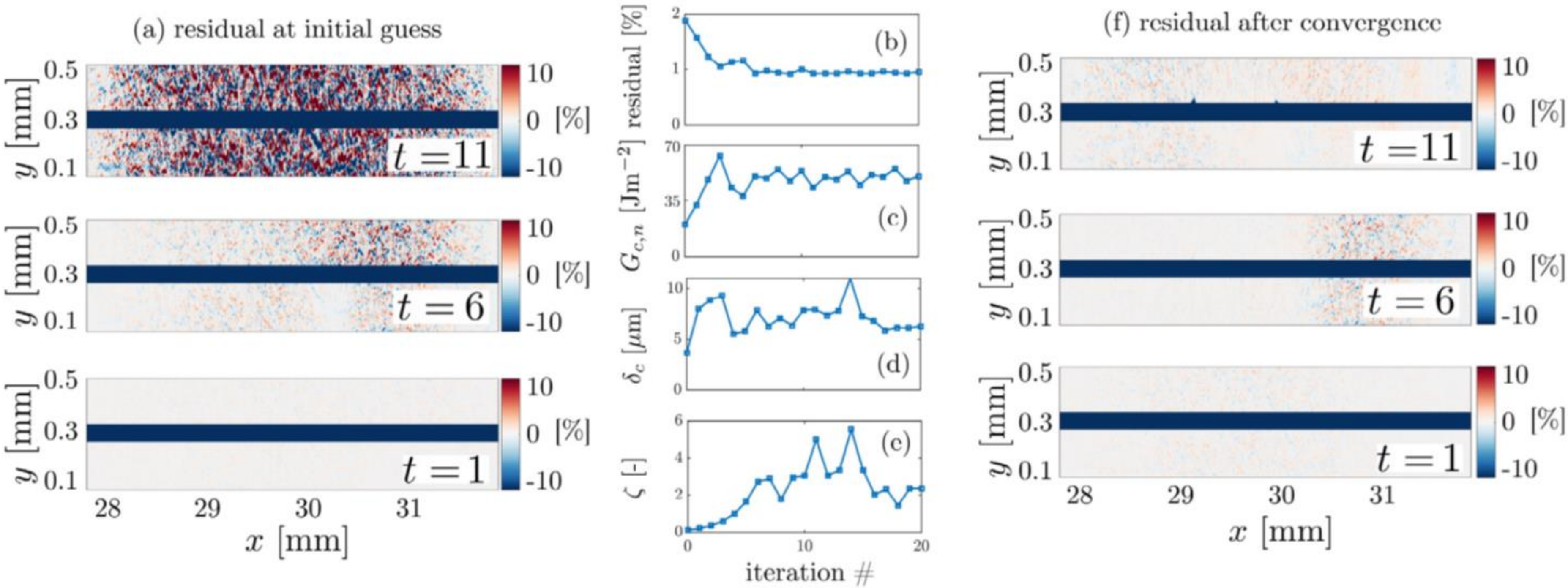

Technische Universiteit Eindhoven University of Technology

/ Mixed-mode: Real Experiments

Real experiments

$G_{c,n}$ = 44 ± 4 Jm^{-2}

$\bar{G}_{c,n} = 49.8 \pm 4.0\ \mathrm{Jm}^{-2}$
$\bar{\delta}_c = 7.3 \pm 1.4\ \ \mu\mathrm{m}$
$\bar{\zeta} = 3.3 \pm 1.3\ \ [-]$

Different mode-mixity: $\xi = 0.0, 0.25, 0.5, 0.63$

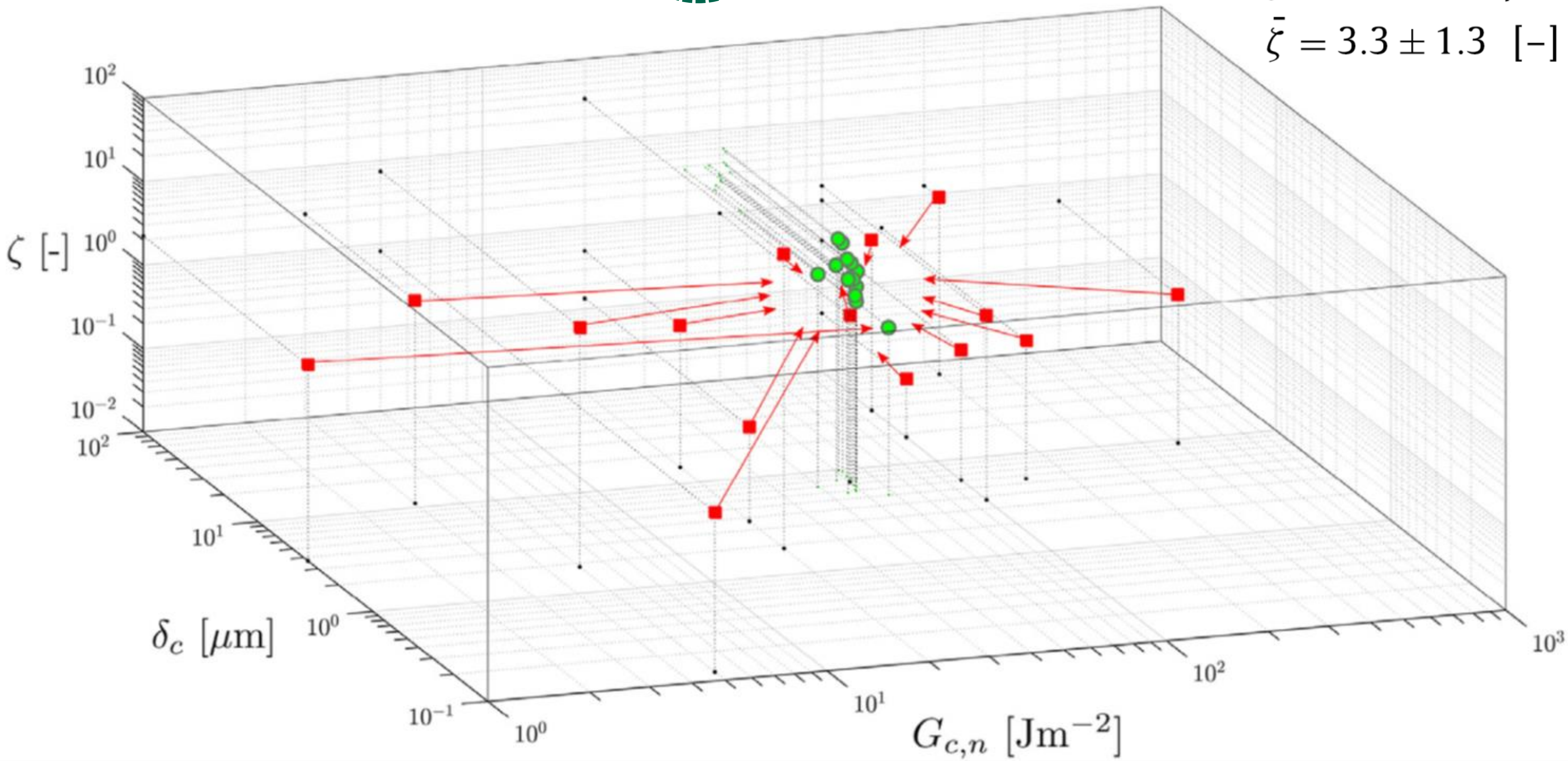

➔ identification of mixed-mode CZ model from a **single** mixed-mode test using micrographs only !

/ IDIC: Mixed-mode interface identification from movie only

Real experiments

- Industrial test case:
  - Delamination in multi-layer moisture barrier for protection of flexible OLEDs (organic light-emitting diodes)

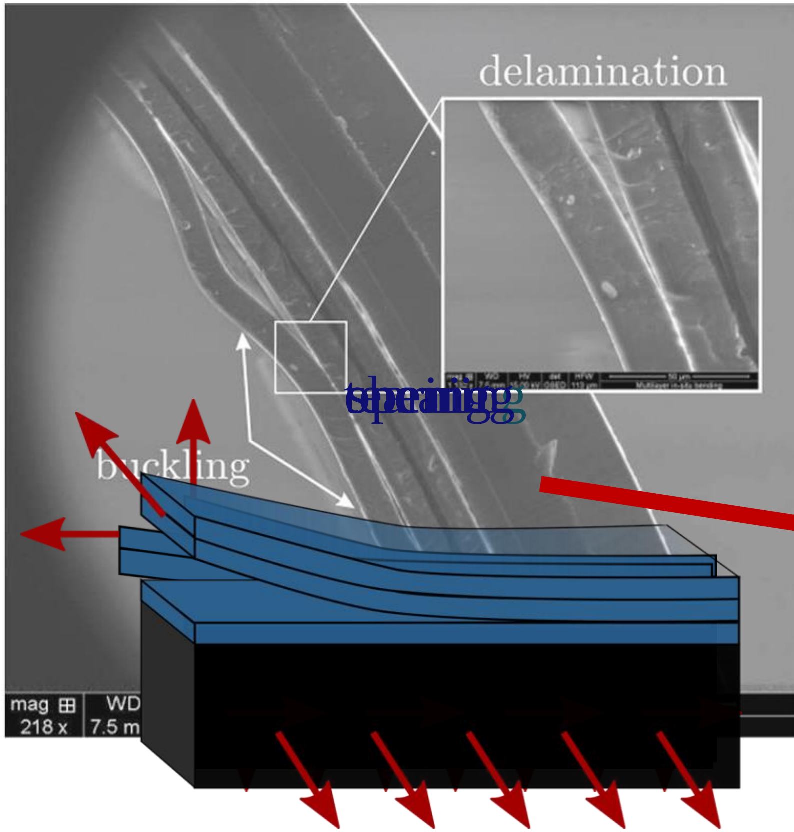

- Novel multi-axial mechanical testing apparatus:

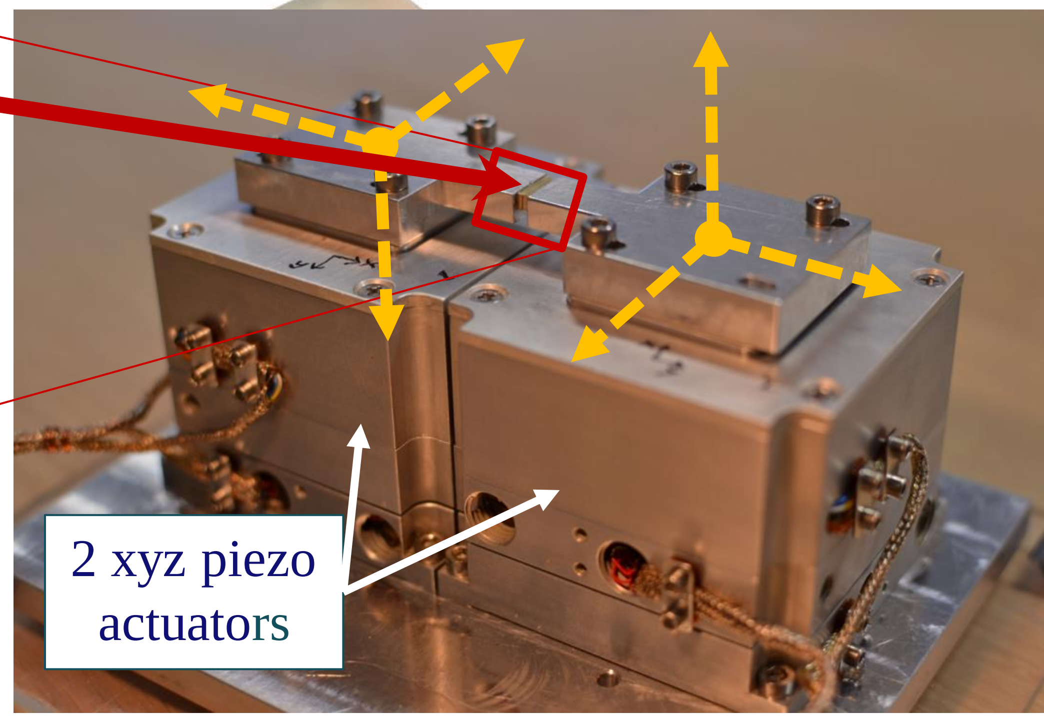

- nanometer resolution
- multi-directional loading
- 3D force sensing
  - (not used here)

- Challenge 1: Local BC optimized, in virtual experiments

Virtual experiments

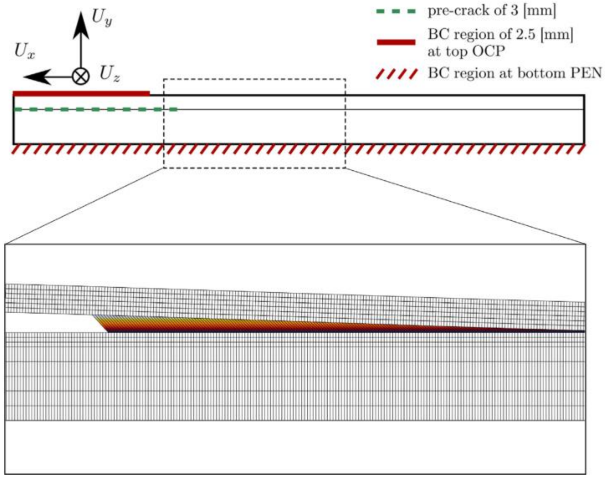

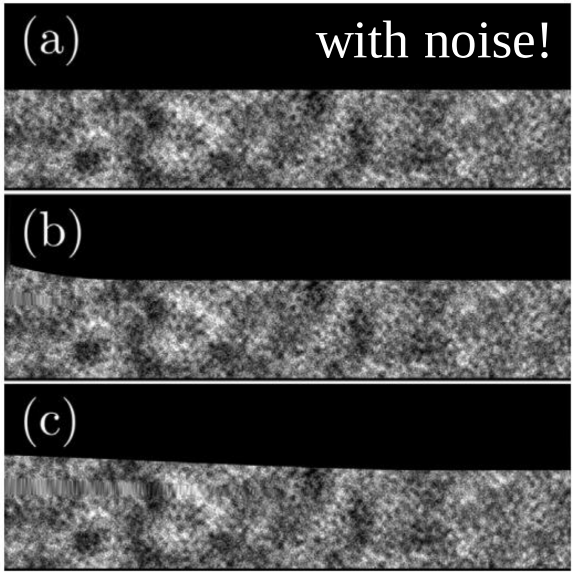

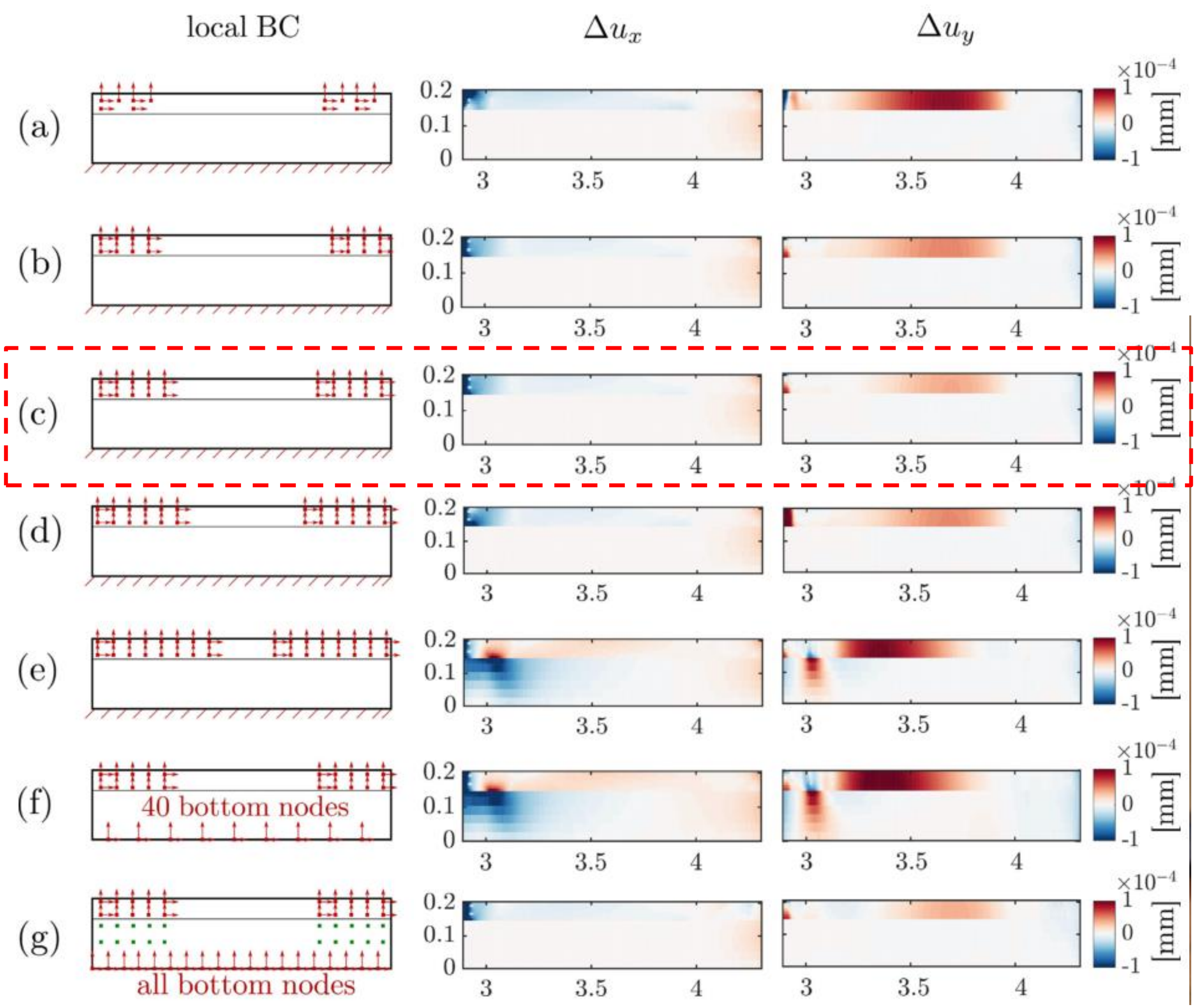

Ruybalid, Hoefnagels, v.d. Sluis, Geers, Eng.Fract.Mech. (2020)

Virtual experiments

- Challenge 1: Local BC optimized, in virtual experiments
- Challenge 2: Loading conditions optimized for maximum parameter sensitivity:

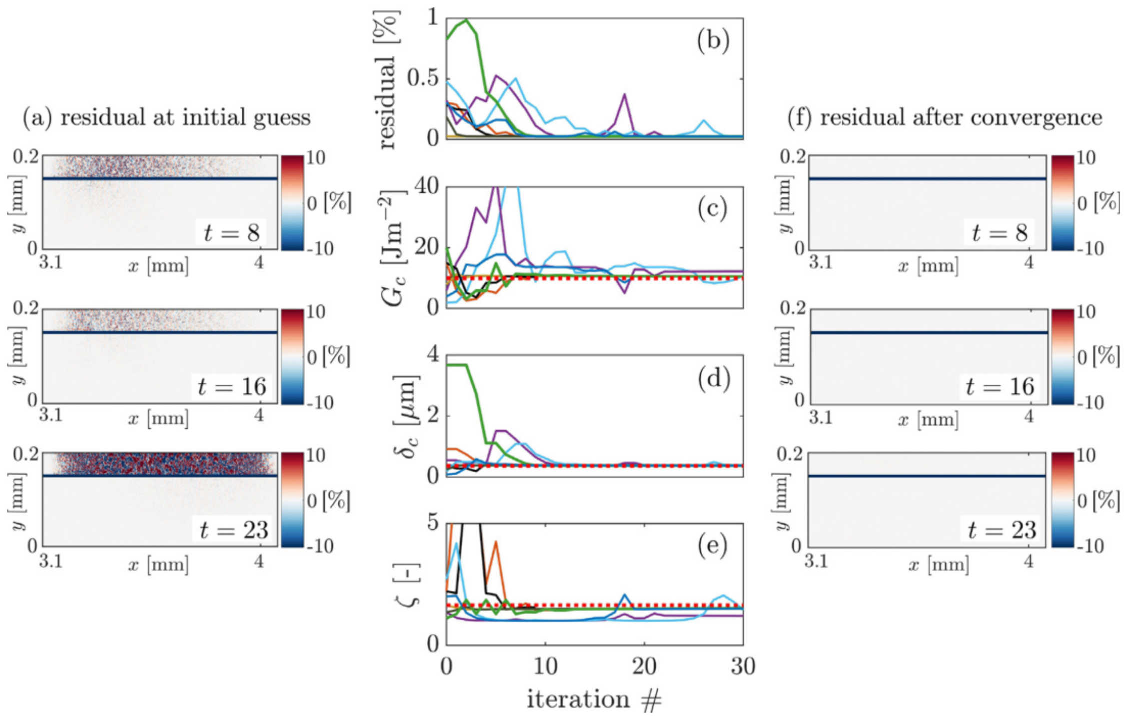

	Load-case (d)
$G_{c,n}$ [Jm^{-2}]	10.60
$\epsilon_{G_{c,n}}$ [%]	6.00
δ_c [μm]	0.378
ϵ_{δ_c} [%]	2.66
ζ [–]	1.51
ϵ_ζ [%]	– 8.41

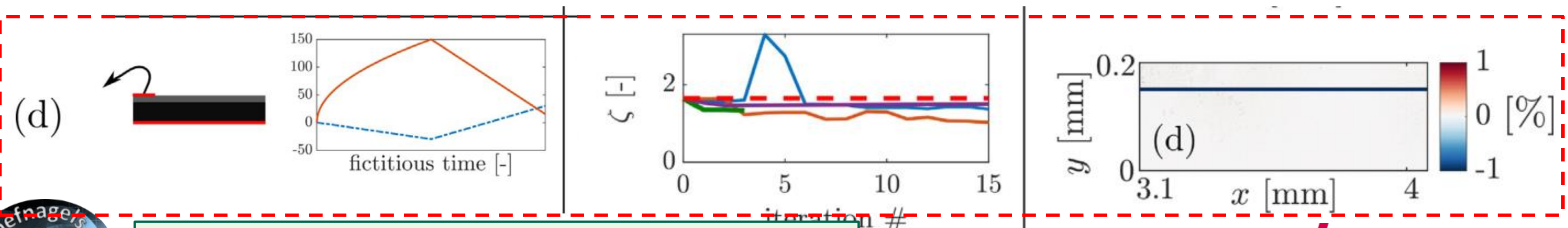

Ruybalid, Hoefnagels, v.d. Sluis, Geers, Eng.Fract.Mech. (2020)

Real experiments

- Challenge 1: Local BC optimized, in virtual experiments
- Challenge 2: Loading conditions optimized for maximum parameter sensitivity:

Eigen value decomposition of Hessian matrix:

$M = QDQ^T$

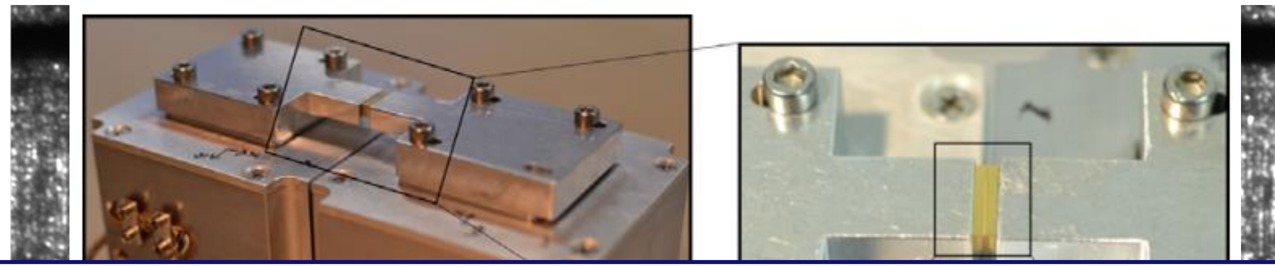

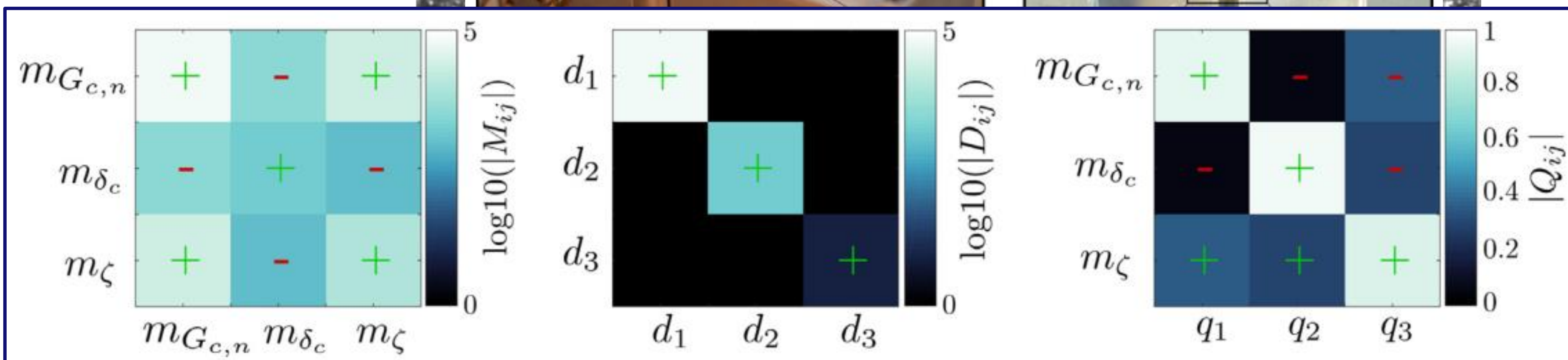

(d)

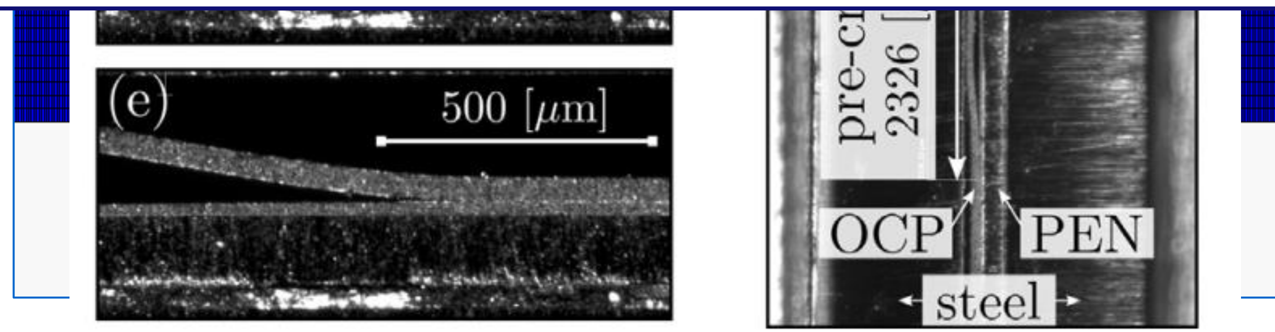

/ IDIC: Mixed-mode interface identification from movie only

Real experiments

- Challenge 1: Local BC optimized, in virtual experiments
- Challenge 2: Loading conditions optimized for maximum parameter sensitivity:
  - ➔ Convergence to global minimum
  - ➔ $G_{c,n} = G_{c,t}$ ← organic layer

$$G_{c,n} = 7.17 \pm 0.07 \ \ [\mathrm{Jm}^{-2}]$$
$$\delta_c = 0.419 \pm 0.014 \ \ [\mu\mathrm{m}]$$
$$\zeta = G_{c,t}/G_{c,n} = 1.001 \pm 0.001 \ \ [-]$$

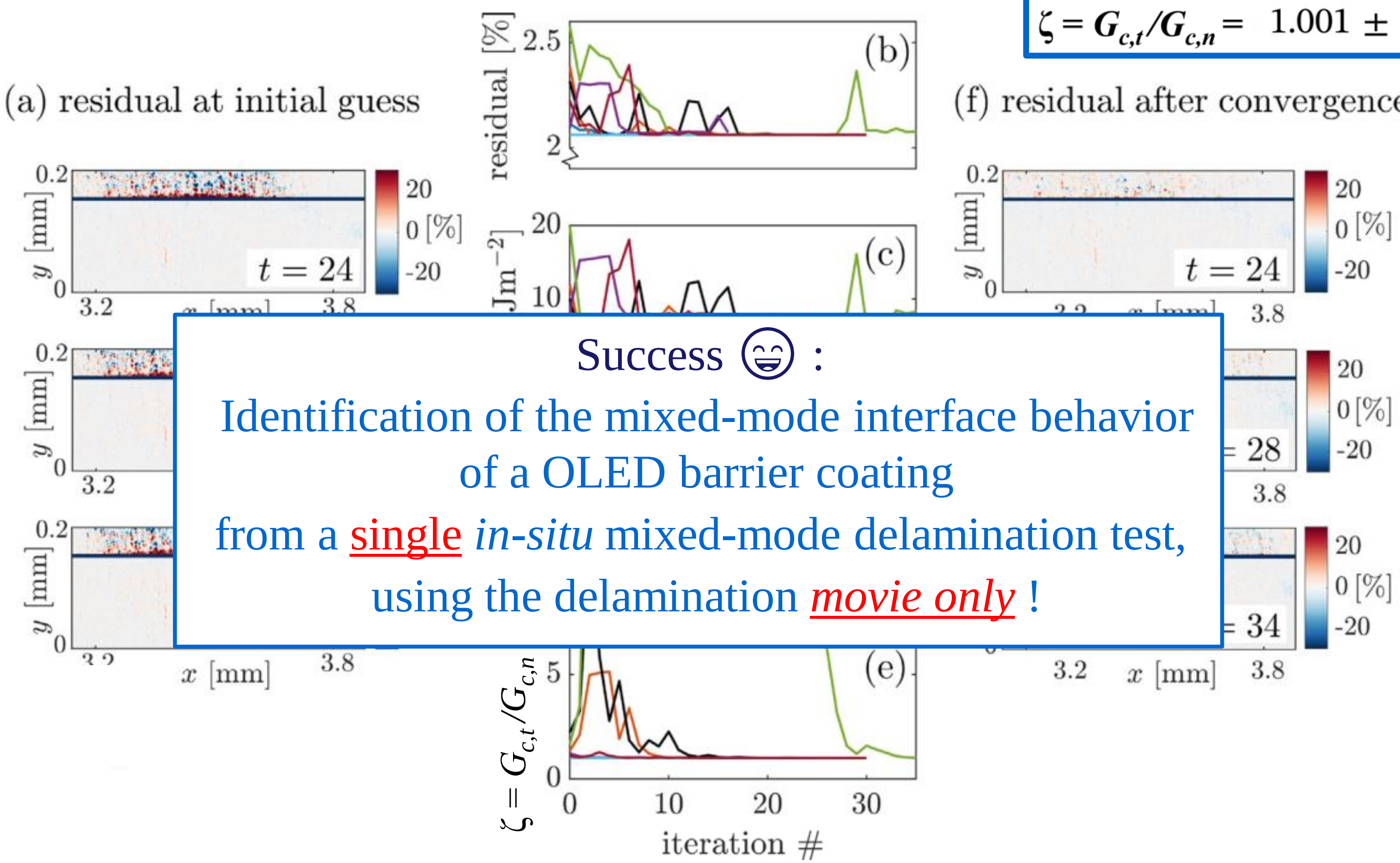

Success 😁 :
Identification of the mixed-mode interface behavior of a OLED barrier coating
from a <u>single</u> *in-situ* mixed-mode delamination test,
using the delamination <u>*movie only*</u> !

Ruybalid, Hoefnagels, v.d. Sluis, Geers, Eng.Fract.Mech. (2020)

European Research Council

Established by the European Commission

Netherlands Organisation for Scientific Research

FOM

materials innovation institute

PHILIPS

Full-field identification of mixed-mode adhesion properties in microelectronics from micrographs only

Johan Hoefnagels,

Andre Ruybalid, Olaf van der Sluis, & Marc Geers

dept. Mechanical Engineering

Eindhoven University of Technology, NL

j.p.m.hoefnagels@tue.nl

www.tue.nl/hoefnagels-group

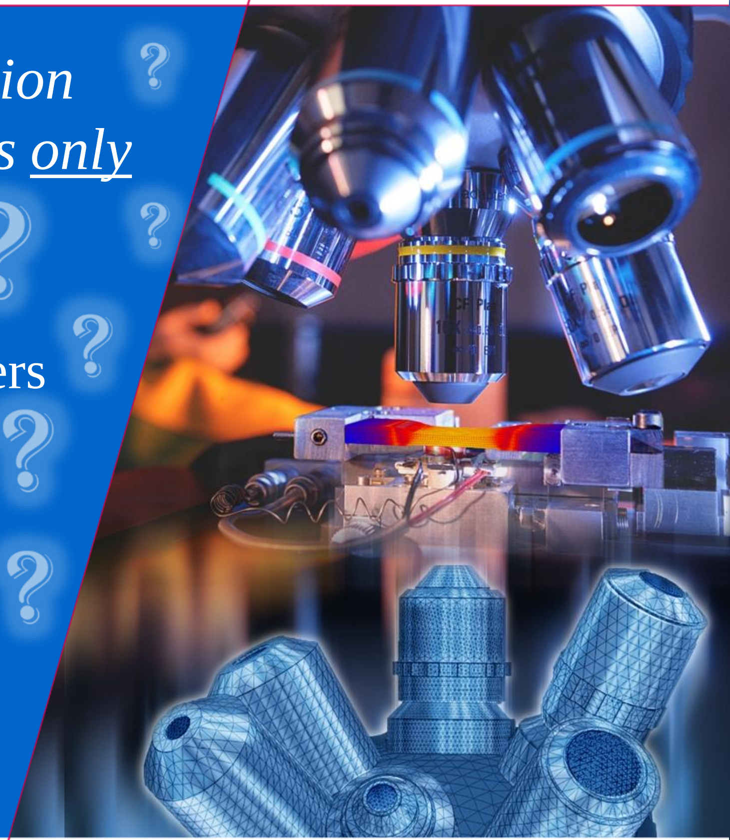

Ruybalid et al. IJSS (2018); Ruybalid et al. IJSS (2019); Ruybalid et al. Exp.Mech. (2020); Ruybalid et al. Eng.Frac.Mech. (2020)

Hoefnagels group

eindhoven university of technology

Where innovation starts

/ Integrated Digital Image correlation (IDIC)

Neggers *et al.*, Jnt. J. Sol. Struct. (2016)

$$f(\underline{x}) \approx g \circ \underline{\phi}(\underline{x}, \mathbb{a})$$

$$\Psi(\mathbb{a}^k) = \frac{1}{2}\int_\Omega \left[f(\underline{x}) - g \circ \underline{\phi}(\underline{x}, \mathbb{a}^k)\right]^2 \mathrm{d}\underline{x}$$

One-step linearization:

$$\forall i \in [1, n], \quad \Gamma_i(\mathbb{a}^{\text{opt}}) = \frac{\partial \Psi}{\partial a_i}(\mathbb{a}^{\text{opt}}) = 0$$

$$\mathbb{a}^{k+1} = \mathbb{a}^k + \delta\mathbb{a},$$

$$\mathbb{M} \cdot \delta\mathbb{a} = \mathbb{b} \quad \text{with} \begin{cases} \mathbb{M} = \begin{bmatrix} M_{11} & \dots & M_{1j} & \dots & M_{1n} \\ \vdots & & \vdots & & \vdots \\ M_{i1} & \dots & M_{ij} & \dots & M_{in} \\ \vdots & & \vdots & & \vdots \\ M_{n1} & \dots & M_{nj} & \dots & M_{nn} \end{bmatrix}, \text{and } M_{ij} = \frac{\partial \Gamma_i}{\partial a_j}(\mathbb{a}^k) \\ \mathbb{b} = [b_1, b_2, \dots, b_n]^T, \text{ and } b_i = -\Gamma_i(\mathbb{a}^k) \end{cases}$$

$$\forall i \in [1, n], \quad \Gamma_i(\mathbb{a}^{k+1}) = 0 \Rightarrow \Gamma_i(\mathbb{a}^k) + \frac{\partial \Gamma_i}{\partial \mathbb{a}}(\mathbb{a}^k)\delta\mathbb{a} = 0$$

$$\forall i \in [1, n], \quad \frac{\partial\left[g \circ \underline{\phi}\right]}{\partial a_i} = \underbrace{\frac{\partial \underline{\phi}}{\partial a_i}}_{=\underline{\varphi}_i} \cdot \underbrace{\underline{\text{grad}}(g) \circ \underline{\phi}}_{=\underline{G}}$$

$$\forall i \in [1, n], \; b_i = -\int_\Omega \underline{\varphi}_i(\underline{x}, \mathbb{a}) \cdot \underline{G}(\underline{x}, \mathbb{a})\, r(\underline{x}, \mathbb{a}) \mathrm{d}\underline{x}$$

$$M^a_{ij} = \int_\Omega \underline{\varphi}_i(\underline{x}, \mathbb{a}) \cdot \underline{G}(\underline{x}, \mathbb{a})\, \underline{G}(\underline{x}, \mathbb{a}) \cdot \underline{\varphi}_j(\underline{x}, \mathbb{a})\, \mathrm{d}\underline{x}$$

/ Integrated Digital Image correlation (IDIC)

Ruybalid, Hoefnagels, v.d. Sluis, Geers, Eng.Fract.Mech. (2020)

The three cohesive zone parameters of interest are identified by integrated digital image correlation (IDIC) [22,31,33]. For the problem addressed here, the residual difference between a reference image of the undeformed material configuration and images of the deformed material configurations is minimized, using the displacement fields from the finite element simulations:

$$\Psi = \int_\tau \int_\Omega \frac{1}{2}\left(f(\vec{x}, t_0) - g\circ\vec{\phi}(\vec{x}, t, \theta_i)\right)^2 \mathrm{d}\vec{x}\,\mathrm{d}t, \tag{3}$$

where f and g are the scalar intensity fields of the reference configuration at time t_0 and the deformed configurations at time t, respectively. Furthermore, the symbol $\circ$ denotes a function composition. Image g is a function of the mapping function $\vec{\phi}$ that maps the pixel position vector $\vec{x}$ in image f to the pixel position vector in image g [27] by:

$$\vec{\phi}\left(\vec{x}, t, \theta_i\right) = \vec{x} + \vec{h}\left(\vec{x}, t, \theta_i\right), \tag{4}$$

using the displacement field $\vec{h}\left(\vec{x}, t, \theta_i\right)$ from the finite element simulation, incorporating the cohesive zone model of [Eq. (1)] with its model parameters $\theta_i = [\theta_1, \theta_2, ..., \theta_n]^T$ (where n is the total number of unknown parameters). Using the Gauss–Newton method, the square image residual of [Eq. (3)] is minimized for all pixels in the space domain Ω and the time domain τ by optimizing the model parameters in an iterative fashion:

$$\frac{\partial\Psi}{\partial\theta_i} = 0, \tag{5}$$

yielding a linear system of equations:

$$M_{ij}\delta\theta_j = b_i, \tag{6}$$

where the correlation matrix M_{ij} and the right-hand side b_i are:

$$\forall\ (i) \in \left[1, n\right], b_i = \int_\tau \int_\Omega \vec{H}_i\left(\vec{x}, t, \theta_i\right)\cdot\vec{G}\left(\vec{x}, t, \theta_i\right)\left(f(\vec{x}, t_0) - g\circ\vec{\phi}(\vec{x}, t, \theta_i)\right)\mathrm{d}\vec{x}\,\mathrm{d}t, \tag{7}$$

$$\forall\left(i, j\right) \in [1, n]^2, M_{ij} = \int_\tau \int_\Omega \vec{H}_i\left(\vec{x}, t, \theta_i\right)\cdot\vec{G}\left(\vec{x}, t, \theta_i\right)\vec{G}\left(\vec{x}, t, \theta_i\right)\cdot\vec{H}_j\left(\vec{x}, t, \theta_j\right)\mathrm{d}\vec{x}\,\mathrm{d}t, \tag{8}$$

The gradient $\vec{G}$ is here taken to be the spatial gradient of the reference image f, but different choices are possible [27]. Furthermore, $\vec{H}_i$ represent the kinematic sensitivities of the simulated displacement fields $\vec{h}\left(\vec{x}, t, \theta_i\right)$ with respect to each parameter θ_i:

$$\vec{H}_i\left(\vec{x}, t, \theta_i\right) = \frac{\partial\vec{h}\left(\vec{x}, t, \theta_i\right)}{\partial\theta_i}, \tag{9}$$

which are here calculated by a forward finite difference approach that requires the model response for a parameter set and the perturbed model responses for each perturbed parameter. In practice, this means that $n + 1$ simulations must be run for each iteration of the IDIC routine. Although other optimization schemes are possible, as explored in [17], the Gauss–Newton method provides a good balance between accuracy and robustness [27].